Analytica Chimica Acta 1355 (2025) 343894

Contents lists available at ScienceDirect

Analytica Chimica Acta

journal homepage: www.elsevier.com/locate/aca

Shear flow deformability cytometry: A microfluidic method advancing towards clinical use - A review

Lija Fajdiga [a], Špela Zemljič [a], Tadej Kokalj [b,*], Jure Derganc [a,**]

[a] Institute of Biophysics, Faculty of Medicine, University of Ljubljana, Vrazov trg 2, 1000, Ljubljana, Slovenia
[b] Institute of Metals and Technology, Lepi pot 11, 1000, Ljubljana, Slovenia

HIGHLIGHTS

- Deformability cytometry is a high-throughput microfluidic method for cell analysis.
- It provides mechanical and morphological phenotyping of suspended cells.
- Its applications with blood cells and tissue cells are reviewed.
- Challenges on its way to clinical adoption are discussed.

GRAPHICAL ABSTRACT

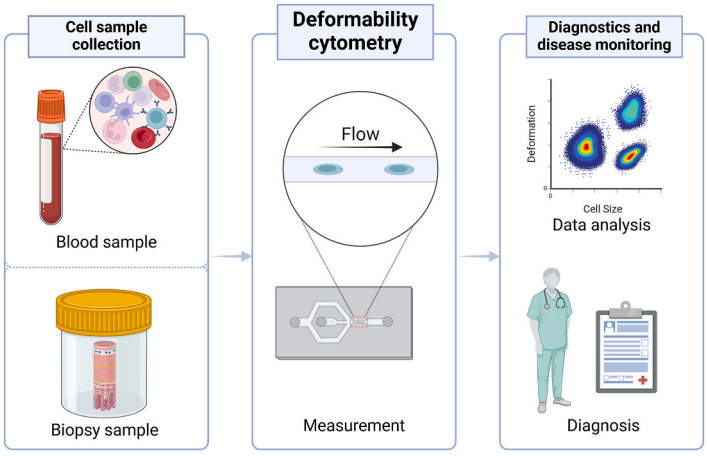

ARTICLE INFO

Keywords:
Deformability cytometry
Microfluidics
Cell mechanics
Mechanical biomarkers
Blood analysis
Disease
Single-cell
Clinical method

ABSTRACT

Background: Shear flow deformability cytometry is an emerging microfluidic technique that has undergone significant advances in the last few years and offers considerable potential for clinical diagnostics and disease monitoring. By simultaneously measuring mechanical and morphological parameters of single cells, it offers a comprehensive extension of traditional cell analysis, delivering unique insight into cell deformability, which is gaining recognition as a novel biomarker for health and disease. Due to its operating principle, the method is particularly suitable for the clinical analysis of blood samples.
Results: This review focuses on the recent developments in shear flow deformability cytometry, which is a widely adopted variant of deformability cytometry. It has a strong potential for applications in clinical practice due to its robust and simple operation, demonstrated applications with whole blood samples, as well as its high throughput, which can reach approximately 1000 cells per second. We begin by discussing some basic factors that influence the mechanical properties of cells and give an overview of deformability cytometry and its operational principles for samples from blood, cultured cells and tissues. Next, we review recent clinically

* Corresponding author.
** Corresponding author.
E-mail addresses: tadej.kokalj@imt.si (T. Kokalj), jure.derganc@mf.uni-lj.si (J. Derganc).

https://doi.org/10.1016/j.aca.2025.343894
Received 12 December 2024; Received in revised form 20 February 2025; Accepted 3 March 2025
Available online 4 March 2025

relevant applications in analysis of blood and cancer cells. Finally, we address key challenges to clinical adoption, such as regulatory approval, scalable manufacturing, and workflow integration, emphasizing the need for further validation studies to facilitate clinical implementation.

Significance: This article uniquely emphasizes the clinical relevance of microfluidic shear flow deformability cytometry, by giving an overview of mechanical and morphological biomarkers studied in clinically significant samples. In addition, it addresses critical barriers to clinical translation. By identifying these obstacles, this article aims to demonstrate the potential of deformability cytometry to bridge the gap between the research and the routine medical practice.

1. Introduction

Blood tests are fundamental tools in clinical diagnostics, providing one of the most important insights into a patient's health. Traditional biochemical tests focus on plasma concentrations of analytes such as glucose or cholesterol, but significant diagnostic value also lies in the analysis of individual blood cells, for example in counting white blood cells of different subtypes. However, robust and accurate high-throughput analysis of individual cells, crucial for effective clinical tests, is technically challenging.

A clinical breakthrough that replaced the labor-intensive manual inspection of cells under the microscope came in the late 1950s with the introduction of automated cell counters based on the Coulter principle, which measures the impedance of individual cells [1]. In the 1970s, cell counters were joined by flow cytometers, which excel at high throughput and the detection of multichannel fluorescence signals and have become an indispensable tool for the characterization of cell surface receptors in hematology and immunology [2]. Modern automated clinical cell counters combine several types of measurements in the now routine clinical test called the complete blood count (CBC), providing information on numerous blood parameters of platelets, red blood cells and the main classes of white blood cells.

New candidates for blood-based biomarkers that could extend standard clinical blood tests are being discovered on an almost daily basis [3, 4]. However, the path of a biomarker from the research laboratory to the clinical setting is not an easy one. One example of such a biomarker is cell deformability, which has been shown to change not only in response to disease but also during functional processes, such as white blood cell

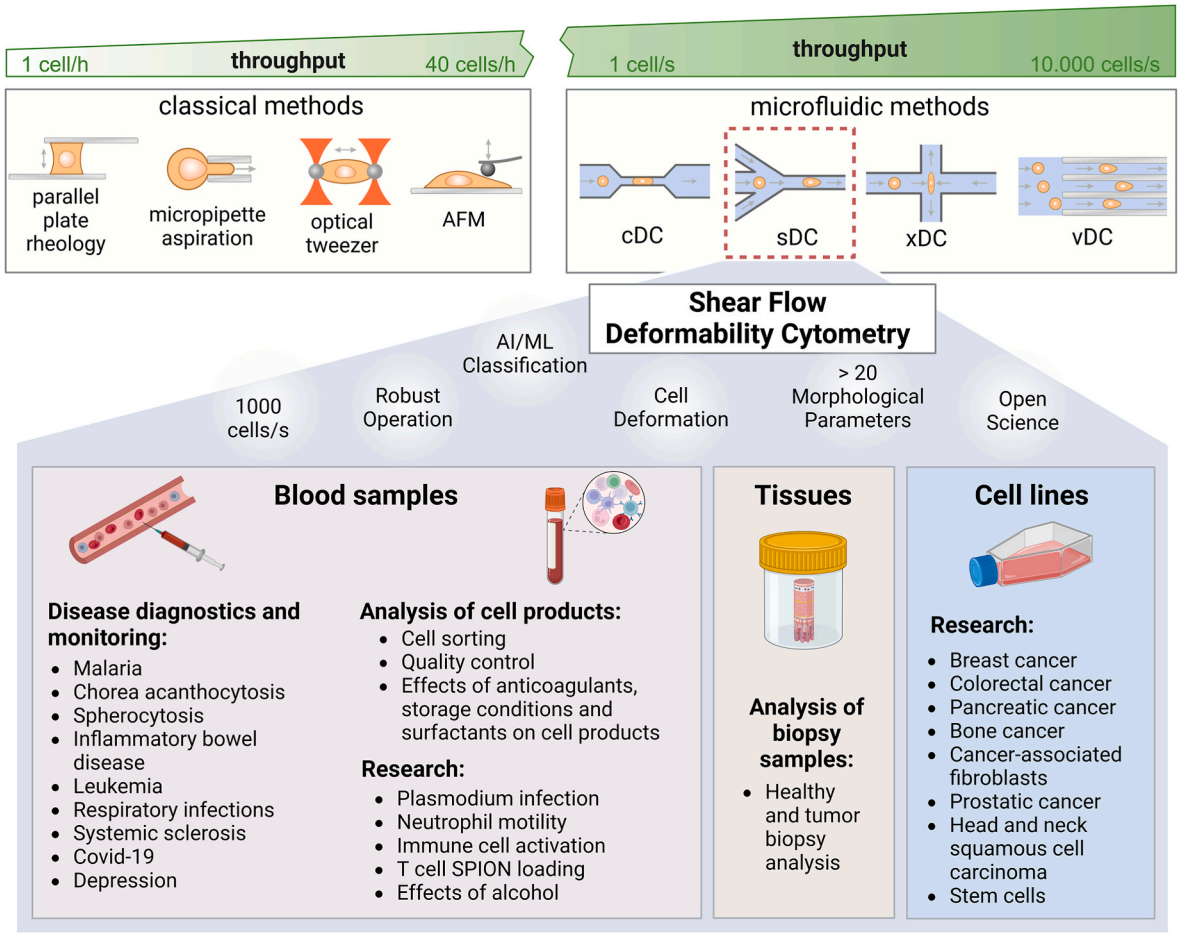

Fig. 1. Overview of Shear Flow Deformability Cytometry (sDC). Among classical and microfluidic methods for measuring the mechanical properties of individual cells, sDC stands out for its broad range of applications with strong clinical potential. It is a robust, user-friendly technique developed largely under open science principles. Like all microfluidic methods, sDC offers significantly higher throughput than classical approaches, processing up to 1000 cells per second while measuring cell deformation and over 20 morphological parameters. These features enable powerful AI/ML-based cell classification. Its applications include analyzing blood samples (whole blood and isolated blood cells), tissue cells from biopsies with clinical relevance, and cultured cells for basic research. Created in BioRender. Derganc, J. (2025) https://BioRender.com/z18e884.

activation [5,6].

Several experimental methods have been developed to assess individual cell deformability, including micropipette aspiration, atomic force microscopy, optical stretching, and magnetic and optical tweezers [7,8]. However, these classical methods have a low throughput as they are relatively labor-intensive, require extensive training for the operators, and have thus remained predominantly in the domain of research laboratories [9]. One notable exception is ektacytometry, which uses light scattering on erythrocytes under defined shear stress in a rotating cuvette. However, it measures only the average deformability for the entire cell population and its use is largely limited to the diagnosis of specific erythrocyte disorders, such as sickle cell disease [10].

Accurate measurements of individual cell deformability have been catalyzed by recent advances in microfluidic techniques [11–14]. Unlike classical techniques, microfluidic approaches are limited to measuring suspended cells, but they offer a crucial advantage for clinical applications: significantly higher throughput. While classical techniques analyze at most a few cells per hour, microfluidic methods can measure up to several thousand cells per second. Using analogy with high-throughput flow cytometry, these microfluidic techniques are commonly referred to as *deformability cytometry* (DC) (Fig. 1 and Table 1).

Historically, the first DC methods analyzed the passage of cells through capillary-mimicking channels that are narrower than the cells themselves, a technique known as *constriction-based deformability cytometry* (cDC). In such a setup, cell stiffness can be inferred from the metrics such as transit time through the narrowing [15–17], the pressure drop [18], cell elongation or impedance [16]. However, very narrow channels significantly increase the chance of clogging the microfluidic system, which is not acceptable in a clinical device.

Alternative DC approaches have therefore employed contactless cell deformation based on hydrodynamic forces exerted on the cells by the carrier medium in channels that are wider than the cell diameter (Fig. 1, Table 1). In *extensional flow deformability cytometry* (xDC) the cell deformation is a consequence of extensional flow in a cross-shaped channel [19–23]. In *shear flow deformability cytometry* (sDC), the cells are focused by a sheath flow into a narrow channel where they are deformed by shear and compression forces exerted by the carrier buffer [24]. Most recently, *viscoelastic deformability cytometry* (vDC) has been introduced, where the cells are deformed by forces exerted in a viscoelastic medium [25]. Due to facilitated cell focusing, the latter approach has been successfully parallelized and demonstrates the highest throughput (up to ~10.000 cells/s). In addition, some studies have used variations of DC approaches, e.g., deformation in a pinching flow [26] or by tunable compressive forces [27].

Except for approaches by Reale et al. (2023) [22] and Petchakup et al. (2022) [23], which are impedance-based, the measurement of contactless cell deformability is based on cell imaging, in a similar way to imaging flow cytometry [28]. Therefore, these systems do not only quantify cell deformation, but also provide clear cell images, which are of great value for subsequent cell phenotyping based on cell morphology [29]. Thus, DC holds a great potential to introduce new label-free cell parameters to the standard arsenal of the CBC test.

The many benefits of microfluidic approaches for measuring cell mechanics are described in detail in recent reviews [13,30,31], some of which focus on specific aspects, such as the comparison of different DC methods [32] or the use of computer vision algorithms [33]. This review specifically focuses on the shear flow deformability cytometry (sDC), introduced by the Guck group [24,34], which has demonstrated robust operation on whole blood samples, making it one of the most promising methods for eventual clinical use. Additionally, sDC has been primarily developed based on open-science principles and is already available through at least two commercial providers. Due to its versatility, low cost, and relatively simple operation, sDC has been quickly adopted by many research laboratories for applications ranging from the analysis of cultured cells to the characterization of biopsy samples from tissues (Fig. 1). As of today, among 296 papers on DC, 131 specifically refer to sDC (according to the EuropePMC archive). Furthermore, the technique has already been combined with a fluorescence module [35] or a cell sorting module [36,37]. In this review, we present the fundamental principles of sDC, highlight its primary applications with clinically relevant samples, and provide a critical evaluation of the challenges that must be overcome for its widespread clinical adoption.

2. Principles of deformability cytometry

2.1. Factors influencing cell deformability

The simplest mechanical parameter of a cell is cell deformability, which describes how much a cell passively deforms under external forces and is inversely correlated with cell stiffness and its Young's modulus. In general, cell deformability depends on the interplay

Table 1
Key characteristics of classical and microfluidic methods for measuring the mechanical properties of individual cells.

	Classical methods				
	AFM	Micropipette aspiration	Optical tweezers	Optical stretcher	Parallel-plate rheometry
Throughput (cells/h)	≤40	≤10	≤10	10–100	≤10
Cell state	Adherent	Adherent Suspended	Adherent Suspended	Suspended	Adherent
Buffer	PBS	PBS	PBS	PBS	PBS

Microfluidic deformability cytometry				
	cDC	xDC	sDC	vDC
Throughput (cells/s)	1	1000	Up to 1000	10,000 (real-time) 100,000 (offline)
Cell state	Suspended	Suspended	Suspended	Suspended
Buffer	PBS	PBS 20 % PEG2000 0.5 % MC	0.6 % MC	0.1 % Polyethylene oxide
Cell contact with channel walls	Yes	No	No	No
Analysis	Offline	Offline	Offline or Real-time	Offline or Real-time
Channel width × height (μm)	6 × 15	60 × 30	20 × 20	15 × 15
Mean flow velocity (m/s)	0.01	3.5	0.1	0.7
Commercial providers		Cytovale (US)	Zellmechanik (DE) Rivercyte (DE)	
Open-source analysis (including AI/ML)			https://github.com/DC-analysis https://github.com/maikherbig/AIDeveloper	
Open repositories			https://dcor.mpl.mpg.de/	

between components such as the cell membrane, the cytoskeleton and the cell nucleus [7,30]. The mechanical properties of these components are cell-type specific, as they are closely linked to genetic, epigenetic and biochemical processes. For example, it is well known that many types of cancer cells are less stiff than their normal counterparts [19,38]. In addition, there can be significant differences even within a population of the same cell type due to the physiological and environmental state of the cells [39]. Thus, cell deformability can change during the cell cycle, e.g., in metaphase when nuclear lamina is decomposed, or during activation of immune cells [40].

The most deformable cell type is the erythrocyte, as it has only a thin under-membrane skeleton and lacks a nucleus, making it little more than a "flaccid sack of hemoglobin." For nucleated cell types, deformability depends on all cellular components including the cytoskeleton, which consists of actin microfilaments, intermediate filaments, and microtubules [7]. In suspended cells, a major mechanical component is the active actomyosin network beneath the membrane, which provides cortical tension and drives the cell into a round shape, much like surface tension shapes liquid droplets. Intermediate filaments form an extensive network extending from the nucleus to the plasma membrane, providing bulk structural integrity. Microtubules also spread from the center to the periphery of the cell and provide resistance to compression forces. While the nucleus is primarily important for its role as a regulatory center, it also contributes to cellular stiffness, mainly due to lamin-based intermediate filaments beneath the nuclear envelope and the chromatin that fills the nucleus [41].

Since different cellular structural elements are closely intertwined, disruption of one component often affects all others, making it difficult to separate their functional roles [7,42]. Additionally, because cells are inhomogeneous viscoelastic objects, their mechanical response is highly dependent on both the strain rate and the extent of deformation. As a result, a single experimental method cannot fully capture cell mechanics. To obtain a comprehensive understanding, various complementary techniques have been employed in parallel to probe cells at different deformation levels and strain rates, as well as to assess mechanical properties both locally and at the whole-cell level [43].

For sDC, which probes mechanics at the whole-cell level, typical strain rates are in the order of kHz, with absolute strains reaching up to 20 % [32]. Experiments with sDC have detected altered deformability due to the disruption of nearly all structural elements. For example, sDC has been used to detect membrane cholesterol depletion [44]; disruption of actin filaments using Cytochalasin D, Jasplakinolide, or Latrunculin [45,46]; interference with myosin activity [47], interference with microtubules by Nocodazole and Paclitaxel [46]; and chromatin condensation induced by Trichostatin A, although the latter produced inconsistent results [46]. Methods that exert larger absolute strains, such as cDC and xDC, appear to be more sensitive in assessing the contribution of the nucleus than sDC [48,49].

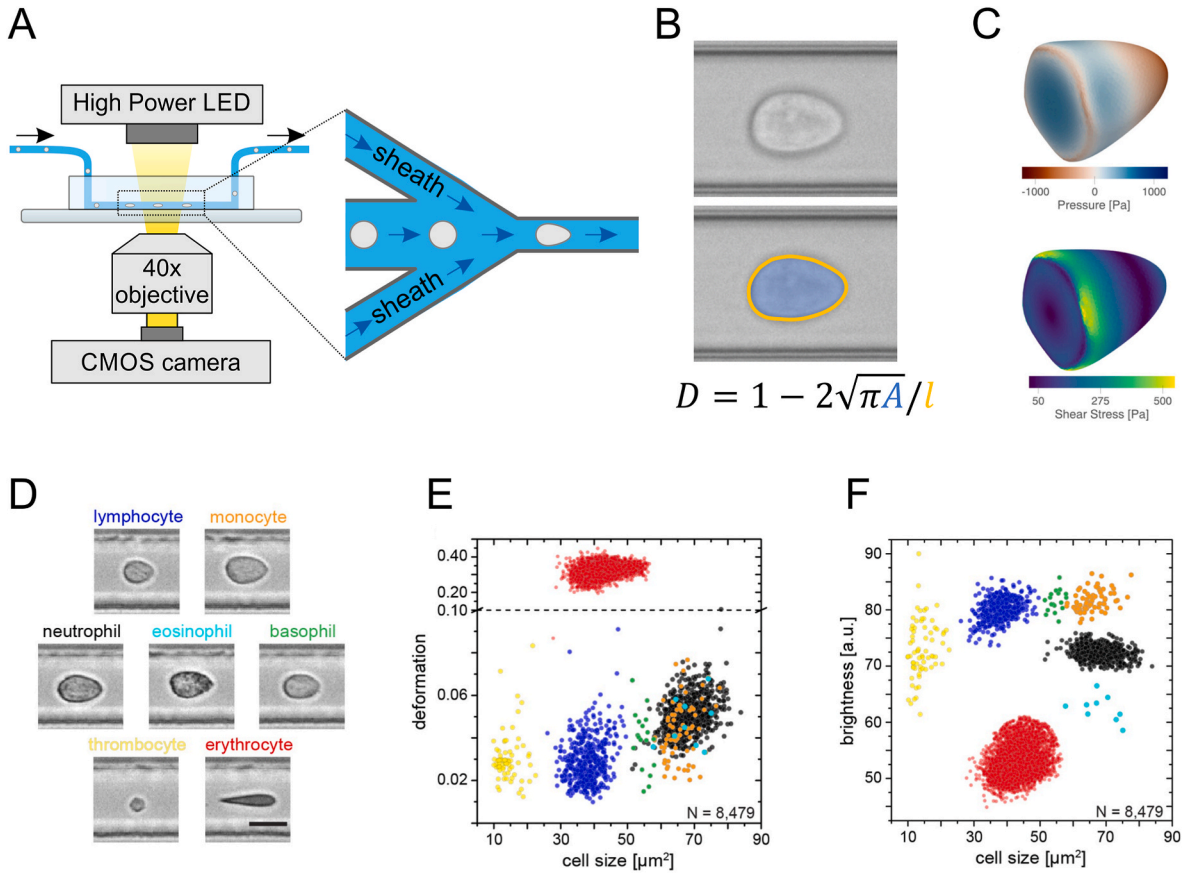

Fig. 2. Operating Principles of Shear Flow Deformability Cytometry. A) Setup for cell imaging in a microfluidic measurement channel - horizontal cross-section is magnified. Using side sheath flow, the cells are focused in a channel narrowing, where they deform under high hydrodynamic forces. B) Typical acquired image of a deformed cell with contour fitting and deformation calculation. C) Calculated hydrodynamic stress exerted on a nucleated cell during a typical experiment: top: pressure, bottom: shear stress. D) Representative images of different blood cell types. More than 20 morphological parameters are measured for each cell. E) Scatterplot of cell deformation (Eq. (1)) versus cell size, which is quantified as cross-sectional area of the image of the deformed cell and is measured in µm^2. F) Scatter plot of average cell brightness versus cell size. On scatter plots, different cell types are revealed as distinct clusters. (Panel C is reproduced from Ref. [50]. Panels D–F are reproduced from Ref. [51], under the terms of the Creative Commons Attribution License (CC BY).

2.2. Basic operation principle of deformability cytometry

One of the main reasons for the widespread use of the sDC is its relatively robust operation and ability to process whole blood samples (Fig. 2). In brief, after the cells are harvested and diluted in the carrier buffer, they are passed through a narrow microfluidic channel with a rectangular cross-section, where they deform under hydrodynamic forces without touching the channel walls. To ensure high enough hydrodynamic forces, the carrier buffer has an increased viscosity by addition of 0.6 % Methylcellulose (MC). During deformation, the cells are imaged with brightfield technique using a standard 40x objective (Fig. 2A) and a fast image acquisition system with custom-made bright illumination. Various cell parameters can be then extracted from the cell images (Fig. 2B). Numerical modeling has shown that in a typical sDC experiment, both types of stress are of the same order of magnitude and that the total stress exerted on cells is approximately 1 kPa [32,34].

The most basic mechanical parameter is the cell deformation, which is determined from the area of its apparent cross section on the image (A) and its perimeter (l), and calculated according to Ref. [34] (Fig. 2B)

$$deformation = 1 - circularity = 1 - 2\sqrt{\pi A}\Big/ l \quad (1)$$

Accordingly, the deformation for cells with a circular cross section is zero and increases with the cell elongation. Deformation is a dimensionless parameter. Note that an alternative and qualitatively similar definition of "deformation" (D) is used in some publications, namely in xDC the deformation is defined as the ratio of the long (a) and short (b) geometrical axis of a cell ($D = a/b$) [19,52].

In a sDC channel, a cell is subjected to two types of stress: hydrodynamic shear stress, which acts tangentially on the cell surface and arises from velocity gradient inside the channel, and hydrodynamic pressure, which acts perpendicularly on the cell surface and results from pressure gradients along the channel (Fig. 2C). Due to exerted forces, nucleated cells deform into a bullet shape, while erythrocytes take on a teardrop shape (Fig. 2D). Along with the cell deformation, several other visual morphologic parameters can be determined, such as the cell size or the average cell brightness (Fig. 2B). Note, that in DC applications, the "cell size" is defined as the area of the image of a deformed cell (cross-sectional area) and is measured in μm^2. When the measured parameters are presented in scatter plots (Fig. 2E and F), specific cell types emerge as distinct clusters. In typical sDC experiments, deformations are less than 0.1 for nucleated cells, and around 0.3 for erythrocytes.

The method is suitable for the processing of up to 1000 cells per second. If the cell analysis is performed instantaneously during image acquisition, sDC is referred to as real-time deformability cytometry (RT-DC). Furthermore, the method can be extended with a laser-based fluorescent module (RT-FDC), which brings its application closer to the standard flow-cytometry [35]. Similarly, the method has been extended with a cell-sorting element (soRT-DC) [36].

Cell deformation in a narrow channel is highly dependent on the channel width, the flow rate, and the viscosity of the carrier buffer. Therefore, these parameters must be precisely controlled to obtain reproducible results. For an optimal performance, the channel width should be just large enough to prevent cells from touching the channel walls. Typically, channels have a square cross-section and are produced with widths ranging from 15 μm to 40 μm. Human blood cells are commonly processed in chips comprising a narrowing with a cross-section of 20 μm × 20 μm [51]. Currently, a single disposable chip made from PDMS costs about 20 $.

To ensure that cell trajectories are centered along the middle of the constricted channel, current sDC systems use hydrodynamic focusing with symmetric side sheath flows (Fig. 2A). The flow rate can be controlled either by syringe pumps or a pressure controller. Syringe pumps provide robust and stable flow control that is less susceptible to potential channel clogging; however, they are cumbersome to use, and it can take several minutes for the flow to stabilize. Pressure controllers are more user-friendly and can stabilize the flow in about 10 s but require coupling with an on-line flow sensor and feedback loop to maintain a constant flow rate in the event of clogging. The basic sDC system occupies no more bench space than a research-grade microscope.

The viscosity of the carrier buffer is typically increased by adding methylcellulose (MC) to 0.6 %, which results in viscosity about 5 mPa s^{-1}. However, since the carrier buffer may interfere with cell properties, it is advisable to mix it with the cells right before the analysis, which then takes about 10 min. Typically, the cell sample solution flow rate is in the range of 0.01 μL/s (the sheath flow is three times as high), so less than 10 μL of cell suspension is needed for one measurement. Even by taking into account the dead volume of the tubing, the minimal required sample volume (cells suspended in carrier buffer) is less then 1 mL.

2.3. Analysis

At the core of sDC measurement is an image-based analysis of individual cells. After an object is detected on the image and its contour is identified, standard mathematical algorithms are applied to calculate various parameters related to the geometrical, morphological, and textural properties of the cell. These parameters include contour perimeter, surface area, deformation (Eq. (1)), porosity, average brightness of the contour's interior and its standard deviation, peak-to-peak brightness, bounding box aspect ratio, Haralick texture features, and more. Open-source software for analysis of these parameters is available on GitHub [53]. Additionally, a sDC device can be equipped with flow cytometer-like functionality using up to three lasers, allowing the image-based features to be augmented by recording fluorescent signals across three channels [35]. In total, over 50 distinct parameters have been described [54], however, only a few have been systematically studied and demonstrated to have predictive value for cell phenotyping.

Cell deformation, as defined by Eq. (1), is not an intrinsic property of the cell, as it is influenced by both cellular stiffness, the ratio of cell size to channel diameter and flow properties. In channels of a given width, smaller cells deform less than larger cells. As previously discussed, cellular stiffness is governed by the complex interplay of various structural components, including the cytoskeleton, membrane, and the nucleus [7]. Nevertheless, as a first approximation, the cell can be modeled as a homogeneous entity, characterized by a single effective parameter, the apparent Young's modulus. It has been shown that differentiating different cell types based on their apparent Young's modulus offers a more robust metric than relying solely on the cell deformation (Fig. 3A and B) [54].

Cell deformation in narrow channels has been modeled in several studies. For example, in the linear regime and with axisymmetric geometry, cell deformations have been shown to be similar whether the cell is modeled analytically as a homogeneous elastic sphere or as a thin elastic shell with surface tension [34]. Subsequently, a more detailed numerical model was developed that incorporated both the stresses in the cell and in the surrounding fluid, and took into account larger deformations with neo-Hookean hyperelasticity [55]. Recently, the neo-Hookean hyperelastic model has been extended to channels with rectangular cross-section (i.e., non-axisymmetric) that more accurately reflect the experimental geometry. Accordingly, new lookup tables have been published, relating deformation and cell size to the apparent Young's modulus (Fig. 3C) [50]. The lookup tables have been incorporated in the open-source software for sDC analysis [53].

Sharp images of individual cells provided by sDC are well-suited for applying machine learning-based methods for feature extraction and cell classification. In fact, several artificial intelligence (AI)-based approaches have already been proposed to analyze sDC data. For instance, Nawaz et al. demonstrated that a simple deep neural network (DNN) can provide fast inference, enabling real-time sorting of neutrophils from erythrocyte-depleted blood [37]. While their DNN was trained on

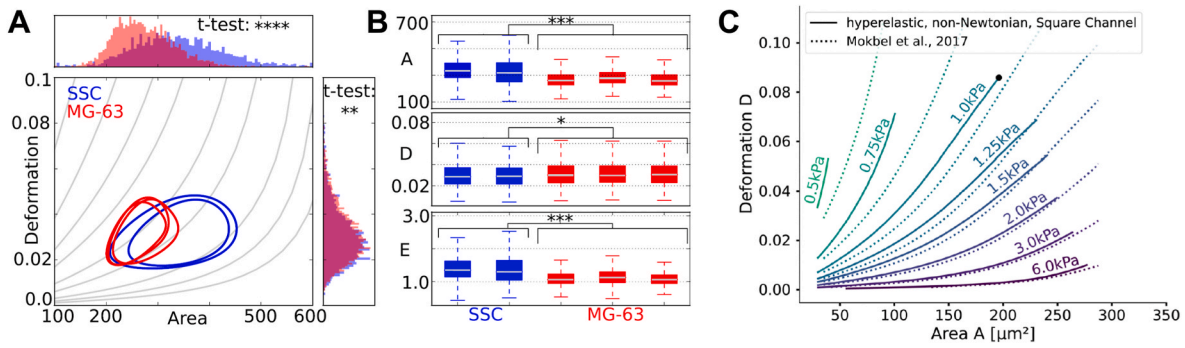

Fig. 3. Assessment of cell effective Young's modulus from calculated iso-elastic lines. A) Contour lines (at 50 % of the maximum density) represent the distributions of two replicates of skeletal stem cells (SSCs) and a triplicate of cells from human osteosarcoma cell line (MG-63) in area and deformation. The grey curves represent isoelasticity lines, obtained from the theoretical model. B) Box-whisker plots for area (A), deformation (D) and the Young's modulus (E) for the same data. The distributions for Young modulus are narrower than for the deformation. The difference between the two cell types is most pronounced for the Young modulus ($p = 2.10 \times 10^{-4}$ vs. $p = 1.25 \times 10^{-2}$ for deformation, and $p = 2.15 \times 10^{-4}$ for area). C) The latest theoretical predictions for isoeasticity lines, calculated within a neo-Hookean hyperelastic model in a square channel. Panels A) and B) are adapted from Ref. [54] under the terms of the Creative Commons Attribution License (CC BY) and panel C) from Ref. [50].

image-derived parameters as well as on fluorescent signals from neutrophil-specific CD66 and CD14 surface markers, the classifier was later able to sort non-stained neutrophils solely based on cell images. Similarly, Ge et al. implemented an unsupervised classifier based on ten image-based features, including area, aspect ratio, and deformation [56]. This allowed them to classify label-free reticulocytes and normal red blood cells, as well as determine the percentage of cells with morphological characteristics of reticulocytes, which are important features for monitoring diseases such as anemia and leukemia.

To support future AI-based studies on sDC data, a comprehensive software package called AIDeveloper was introduced [57]. This tool enabled the first deep learning algorithm capable of classifying blood cells using brightfield images, distinguishing even between B and T lymphocytes. Since then, AI-based label-free cell classification has also been proposed for clinical applications, such as identifying patients with myelodysplastic syndromes [58], and distinguishing platelet aggregates in COVID-19-related thrombosis from non-COVID-19 cases [59].

Classical algorithms for image analysis are sufficiently fast for basic cell detection, contour analysis, and real-time visualization of results at rates of approximately one kilohertz (kHz), even on standard computers [24]. If such real-time analysis is employed, sDC is often referred to as real-time deformability cytometry (RT-DC). However, advanced AI algorithms for cell detection and classification may take more than 1 ms to analyze a single image on a standard computer [58,60], potentially reducing throughput if real-time analysis is required. In many applications, real-time information is unnecessary, and offline analysis after data acquisition is a viable solution. If faster AI-based analysis is required, optimized AI algorithms can reduce inference time to a few hundred microseconds [37,61], or specialized hardware, such as GPUs, can be utilized [37].

3. Cell types analyzed by sDC

sDC has been already extensively used in both clinical and research laboratories for analyzing various cell samples (Tables 2 and 3). For clinical applications, **blood samples** are particularly relevant as the measurement conditions with suspended cells closely resemble physiological conditions *in vivo*. Accordingly, the protocol for the use of sDC for blood analysis is straightforward: after dilution of 50 μL of whole blood in 950 μL of the carrier medium (Fig. 4A), the sample is connected to the microfluidic chip via tubing, and the results are obtained in less than 15 min.

However, with a slightly more complex experimental protocol, **cell lines** and **tissues** can also be studied after the cells have been resuspended (Fig. 4B, C and D). Compared to blood cells, suspension cell lines need to be centrifuged before resuspension in carrier medium (Fig. 2B) and the procedure for adherent cell cultures includes additional detachment by trypsinization (Fig. 2C), adding approximately 30 min to the overall protocol.

In this section we will first focus on clinical samples of blood cells and then consider how sDC can be used to study tissues. The latter has not been extensively studied to date, but the use of the technique for this type of application has been demonstrated using adherent cell lines. They are therefore included in this review. Blood cell lines are not included because the utility of the method has been extensively demonstrated on more clinically relevant primary human blood cells.

3.1. Blood cells

In the clinical analysis of blood, CBC is one of the basic measured characteristics. In 2018, Toepfner and colleagues presented a groundbreaking proof-of-concept study demonstrating the potential of sDC for whole blood analysis using single-cell morpho-rheological phenotyping [51]. They showed that by combining several sDC parameters, such as cell size (cross-sectional area) and average cell brightness, blood cells can be classified into erythrocytes, platelets, neutrophils, lymphocytes, monocytes, eosinophils and basophils (Fig. 2E and F). With this knowledge, sDC can be used to obtain the information normally obtained by CBC but without any cell labeling. In addition, by implementing AI-based approaches, it is now possible to distinguish other cell types such as reticulocytes [56] and even lymphocytes B and T [57]. The latter has not been possible without fluorescent labelling and flow cytometry.

Moreover, as the system assesses cell deformability, it offers further insight into potential functional changes and pathological conditions within the blood cells that may indicate the patient's health status or disease. This information could assist clinicians in narrowing down possible diagnoses and determining the necessity for specific additional tests. Additionally, this method holds promise for monitoring disease progression and treatment efficacy, making it a valuable tool in clinical practice [51].

Studies have already identified various mechanical biomarkers linked to different diseases; however, it is essential to acknowledge that there remains significant untapped potential in this field, and we have only begun to scratch the surface of pathological cell mechanics.

sDC was, for example, shown to identify some of the changes during **maturation and activation of leukocytes**. Bashant and colleagues revealed morpho-rheological changes in neutrophils during activation [89]. Initially, activated neutrophils decreased in size and stiffness, followed by a phase of cell expansion and softening. This implies that

Table 2
Publications on clinically relevant applications of sDC for analyzing human blood or bone marrow samples.

Sample Type	Cell Types	Key Findings	Reference
Whole Blood	RBCs, neutrophils, monocytes, lymphocytes	In severe cases of COVID-19, the number of neutrophils increased, and the number of leukocytes decreased. Red blood cells showed morphological and mechanical changes, lymphocytes were softer, the volume of monocytes was significantly increased, while neutrophils were larger and more deformable, indicating significant changes in the biophysical properties and cell phenotypes of blood cells.	[62]
		Mechanical phenotyping showed changes in red blood cells from patients with spherocytosis, which were smaller and stiffer, and in red blood cells from patients with malaria, which were stiffer. Patients with acute lung injury had larger and more deformable neutrophils, while Epstein-Barr virus infection caused an increase in the deformability and size of monocytes and lymphocytes.	[51]
	RBCs	An increase in the deformability of red blood cells was observed in children and adolescents following infection with SARS-CoV-2.	[63]
	Leukocytes (lymphocytes, monocytes and neutrophils)	Acute alcohol exposure caused decreased stiffness and changes in leukocyte morphology, demonstrating a potential transient effect of alcohol on immune cell mechanics and functionality.	[64]
		Leukocytes became stiffer after exposure to gadolinium-based contrast agents, which could affect their circulation and immune activity.	[65]
	RBCs, neutrophils, monocytes, lymphocytes, granulo-monocytes, thrombocytes	Increased deformability of red and white blood cells was found in patients with depressive disorders, possibly reflecting systemic effects on cell mechanics	[66]
Isolated blood cells	RBCs	Poloxamer 188 (Pluronic F-68) increased the stiffness of red blood cells.	[67]
		Plasmodium falciparum erythrocyte binding induced biophysical changes in red blood cells that increased their deformability, facilitating parasite invasion.	[68]
	Platelets	Platelet deformability was shown to depend on cytoskeletal dynamics, with implications for inherited platelet disorders.	[69]
		Ex vivo anticoagulants induced changes in platelet deformability and size, affecting their functional mechanophenotype.	[70]
		Cold storage reduced platelet deformability, which was restored by treatment with divalent magnesium, which prevented cytoskeletal lesions.	[71]
	T cells	T cells loaded with superparamagnetic iron oxide nanoparticles retained their deformability and antigen-specific T-cell receptor functionality, indicating compatibility with immunotherapies.	[72]
	Regulatory T cells	IL-3 receptor signaling reduced the stiffness of regulatory T cells and increased their egress from tissues, helping to suppress inflammation.	[73]
	Monocyte-derived dendritic cells	Maturation of monocyte-derived dendritic cells increased stiffness, membrane fluidity and altered lipid composition.	[74]
	Chronic lymphocytic leukemia (CLL) cells	Mechanical properties of CLL cells were altered compared to healthy B lymphocytes and could be targeted by BTK inhibitors.	[75]
	PBMCs (monocytes)	Monocytes from patients with systemic sclerosis were stiffer and showed altered morphology.	[76]
Bone marrow	$CD34^+$ hematopoietic stem cells	sDC results were used to build a machine learning model for analyzing hematopoietic stem cells from patients with myelodysplastic syndromes (MDS) and healthy donors. This approach enabled MDS diagnosis. The most important classification feature was cell size distribution, which was broader in patients. The study also suggests that cells with more genetic mutations have lower median deformation and proposes sDC as a promising diagnostic tool for MDS.	[58]

biomechanical properties play an important role in neutrophil trafficking through the circulation. Likewise, significant morphological changes occur within dendritic cells as they migrate to lymph nodes to interact with T cells. In their 2020 study, Lühr and colleagues employed sDC to assess the deformability of immature and mature monocyte-derived dendritic cells (moDC) [74]. Their findings showed that mature cells were stiffer than immature cells even though a significant difference was observed in the composition of the cell membranes, with the membrane of mature moDC being more fluid than that of immature moDC. They proposed that change in mechanical properties could play an important role in migration and T cell activation. Ullrich and colleagues focused their research on IL-3 signaling effect on **T cell** trafficking in **inflammatory bowel disease** patients. They report on elevated levels of IL-3 expression in **colitis** patients, alteration of the actin cytoskeleton and higher deformability of $CD4^+$ T cells exposed to interleukin-3 (IL-3) compared to IL-3 unexposed $CD4^+$ cells. This modulates the migratory capacity and tissue egress of T cells [73].

Erythrocyte pathologies have been analyzed in several studies using sDC. Toepfner and colleagues reported on the potential of deformability cytometry to detect **spherocytosis** as they found that red blood cells are less deformable and smaller than those observed in a normal population (Fig. 5 A) [51]. In a study published in 2022, Reichel and colleagues observed alterations in erythrocyte size and the presence of thorn-like protrusions, but no difference in deformability in patients with **chorea acanthocytosis** [90]. Interestingly, while this hereditary disease is primarily linked to erythrocyte morphology, the researchers also found that it reduced deformability of lymphocytes and myelocytes. The disease treatment also affected red blood cell (RBC) and white blood cell (WBC) deformability. Toepfner and colleagues also observed a decreased deformability of erythrocytes of patients with **malaria** (Fig. 5 B) [51]. Similarly, Koch and colleagues conducted a systematic analysis of biophysical aspects of the infection process, demonstrating that parasite binding to erythrocytes decreases cell deformability and reduces the bending modulus of the cell membrane, thereby facilitating parasite invasion [68]. These studies represent an important advancement in the research of malaria, as until recently the invasion process of *Plasmodium* into the RBCs was focused more on molecular factors.

sDC shows potential in biomechanical analysis of platelets. As with other blood cells, the structural and mechanical properties of platelets play an important role in platelet biogenesis, function and pathology, making them a promising tool for the diagnosis and prognosis of inherited platelet disorders. Their small size also makes the analysis of their mechanical properties difficult, but this is no problem for the sDC method [69]. Zaninetti et al. (2020) observed stiffening of platelets after activation, but when adding Cytochalasin D, platelets remained softer, despite expression of the activation marker [69].

Until recently it was not clear how ex vivo blood collection and processing for clinical use can affect platelet mechanics and with that

Table 3
Publications on clinically relevant applications of sDC for analyzing tissue samples or tissue model cell lines.

Sample Type	Cell Types	Key Findings	Reference
Human tissue	Benign prostate epithelial cells and cancer associated fibroblasts	Cancer-associated fibroblasts (CAFs) exhibited increased stiffness compared to non-malignant prostate tissue fibroblasts. In addition, CAFs induced morphological changes in benign prostate epithelial cells in co-culture.	[77]
	Colorectal cancer patient derived organoids	LGR5+ colorectal cancer stem cells exhibited stiffness, high adhesion to the extracellular matrix, and resilience, supporting metastatic growth, while LGR5- cells were softer, faster, and less adhesive, facilitating invasion and dissemination.	[78]
Human and mouse tissue	Tissue biopsy cells	Physical phenotyping revealed tissue-specific mechanical properties of cells, allowing for a rapid assessment of cellular heterogeneity in mouse tissues. Additionally, it enabled the distinction between tumor and healthy tissue in human biopsies.	[79]
Human tissue, cell lines	Head and neck squamous carcinoma cells and cancer associated fibroblasts	The stiffness and invasive properties of head and neck cancer cells were significantly affected by specific mRNA subtypes of CAFs.	[80]
	Primary human mesenchymal stromal cells, human skeletal stem cells, promyelocytic leukemia cell line (HL-60), osteosarcoma cell line (MG-63)	sDC revealed heterogeneity in stem cell populations and identified subpopulations with distinct mechanical properties.	[81]
Cell lines	Breast cancer cells (MDA-MB-231), enhanced bone-seeking derivative cell lines (MDA-MB-231-MET (MET) and MDA-MB-231-BONE (BONE)), brain-seeking variant (MDA-MB-231-BrM2)	A wide range of cell morphotypes were identified among osteotropic breast cancer cells, which were correlated with molecular, migratory and biophysical properties of the cells. These characteristics may help to predict metastatic potential in breast cancer patients.	[82]
	Pre-invasive breast cancer cells (MCF10A)	Reorganization of actin stress fibers increased cell stiffness and promoted tumor growth in premalignant stages.	[83]
	Breast cancer cells (MCF10A)	Oncogenic signaling pathway changed the shape and reduced the deformability of epithelial cells, facilitating division in confined environments, such as tumors.	[84]
	Breast (MDA-MB-231, MCF7, 4T1 and 67NR), colorectal (SW620 and SW480) pancreatic (KPR172HC and KPflC) cancers cells	Only cancer cells were able to adapt their stiffness in response to the stiffness of the extracellular matrix. Their mechanical properties correlated with increased invasive potential.	[85]
	Breast cancer cells (MDA-MB-231)	Metastatic cells showed increased stiffness and adhesion compared to non-metastatic cells.	[86]
	Osteosarcoma cells (SaOs-2, LM5, HuO9 and M132)	High metastatic potential cells were more deformable compared to low metastatic potential cells.	[87]
	Differentiating cardiomyocytes (iCM, mCM)	The differentiation of cardiac progenitor cells was accompanied by an increase in cell size and stiffness.	[88]

influence their function and bleeding risk in patients. Using sDC, Sachs and colleagues found that **anticoagulants** affect platelet deformability, size and cytoskeletal structure [70]. After isolation, platelet concentrates can be stored at low temperature (4 °C), but this reduces the circulation time of platelets when administered to patients. A significant change in cytoskeletal structure and reduced deformability was observed in cold-stored platelet concentrates. The addition of Mg^{2+} prevented cytoskeletal damage and mechanical changes caused by cold storage [71].

The clinical applications of sDC were investigated also with infectious diseases. For example, Toepfner and colleagues reported on the potential of sDC to detect bacterial and viral infections [51]. They described a clear increase in the deformability and size of neutrophils in patients with acute lung injury resulting from bacterial origin and **viral respiratory infections** (Fig. 5C). In patients with acute **Epstein-Barr virus** (EBV) infection, it was observed that both monocytes and lymphocytes exhibited increased size and deformation, while for neutrophils only a slight change in their deformability was detected and no change in size. During the pandemic, Kubankova et al. (2021) [62] and Eder et al. (2023) [63] compared patients with and without a history of **COVID-19** infection. The former study identified differences in mechanical and morphological markers and cell counts when examining blood samples from patients with COVID-19. The count of neutrophils was significantly elevated, while the count of lymphocytes decreased. Apart from increased deformability of lymphocytes in severe COVID-19 patients, larger monocytes and larger and more deformable neutrophils, they observed a subpopulation of erythrocytes, which were smaller and less deformable than normal population (Fig. 5 D). The distribution of erythrocytes of recovered patients (4 months after COVID-19) did not completely return to normal, which could indicate the effect of long Covid (Fig. 5 D). Eder et al. (2023) focused their study of COVID-19 on RBCs in children and adolescents and observed greater deformability in individuals diagnosed with COVID-19 compared to those who had not been exposed to the virus, but in contrast to the study of Kubankova (2021) in their case, no difference could be observed after 6 months post Covid-19. A comprehensive explanation of the observed phenomena is yet to be provided.

Alterations in leukocyte morphology and biomechanics are hallmarks of **leukemias**. Although cancer cells in solid tumors are known to be more deformable, acute lymphoblastic leukemia (ALL) cells and acute myeloid leukemia (AML) cells were found to be less deformable than healthy cells [51]. Additionally, the blood cells of ALL patients regained their normal morpho-rheological phenotype after 12 days of treatment with methylprednisolone, which suggests that this method could be used for disease monitoring. Sampietro and colleagues

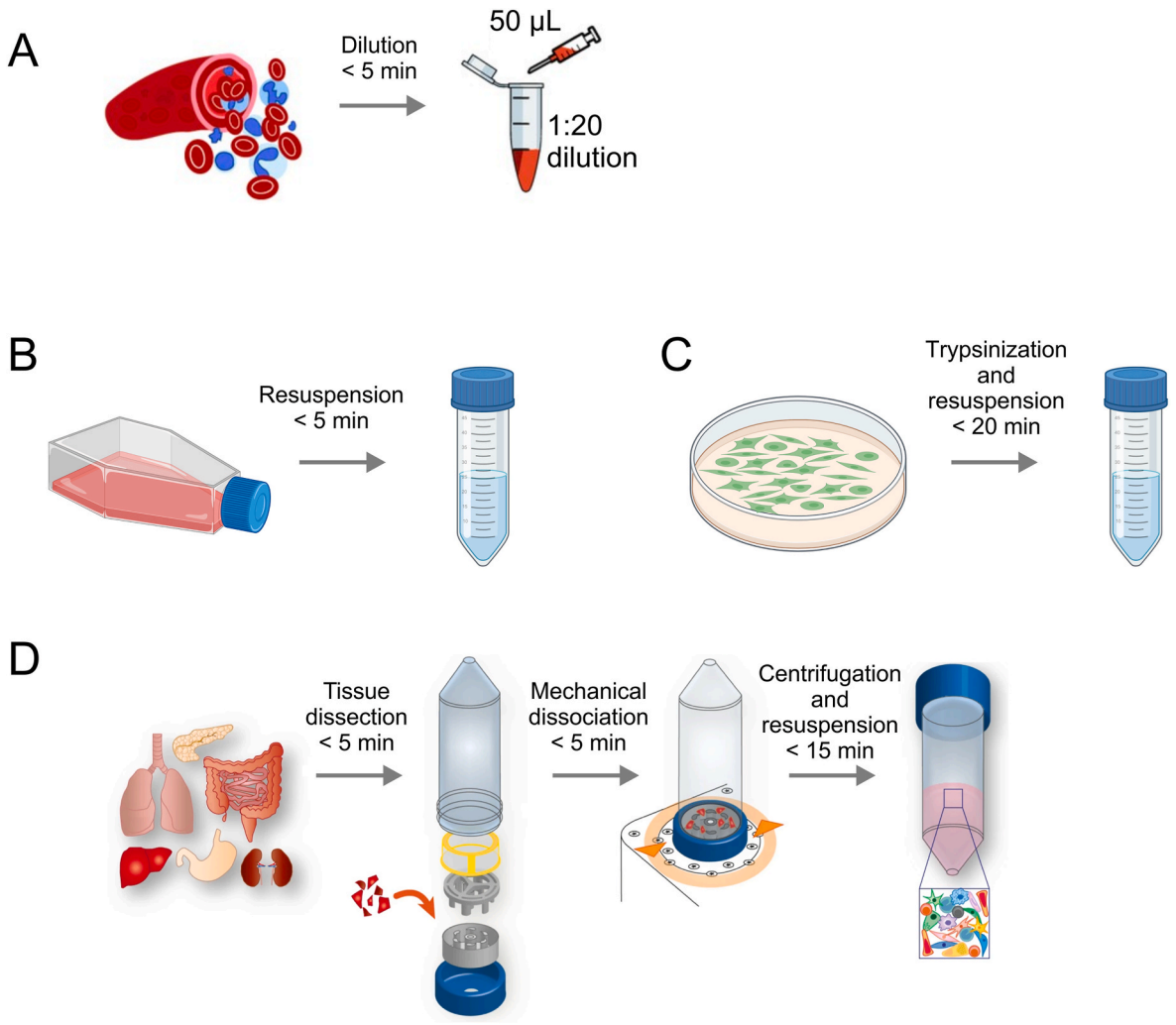

Fig. 4. Schematics of sample preparation for use in sDC. A) Whole blood, B) Culture of suspended cells, C) Adherent cell culture, and C) Tissue. Images are adapted from Refs. [51,79], under the terms of the Creative Commons Attribution License (CC BY).

conducted a comparative analysis of the cytoskeletal structure and mechanical properties of chronic lymphocytic leukemia (CLL) cells and healthy B lymphocytes using sDC [75]. The results demonstrated that CLL cells have a unique actomyosin complex organization and lower deformability compared to healthy B lymphocytes, indicating specific mechanical behavior in leukemia cells. Furthermore, treatment with Bruton's tyrosine kinase (BTK) inhibitors could restore the mechanical properties of CLL cells to a normal phenotype, thereby providing a potential therapeutic target for CLL treatment.

An unexpected area, where sDC proved its clinical potential, are **neurological disorders**, where alterations in blood cells have not been extensively examined previously. Here, Walther and colleagues demonstrated that **depression** can also affect the deformability of specific blood cell types in blood samples from individuals with depression [66].

Matei and colleagues examined the deformation (Young's modulus) and size (cross-sectional area) of immune cells, particularly monocytes, in peripheral blood mononuclear cell (PBMC) samples from patients with **systemic sclerosis** [76]. They proposed that biophysical phenotyping could be a cost-effective alternative to RNA sequencing, mass cytometry and functional assays for disease detection and monitoring.

sDC was also used to assess how changes in the **biochemical environment** affect blood cells. One example is the effect of **ethanol**, which is commonly used in cell culture to solubilize chemicals but may also be relevant in context of human alcohol consumption. Its effect on the mechanical properties of leukocytes was investigated by Shalchi-Amirkhiz et al. [64], who showed that a single drinking session (blood alcohol concentration of 1.2 ‰) didn't affect the deformability of lymphocytes, monocytes and neutrophils from healthy male participants, but it did affect the cell counts and caused a shift towards memory T cells. After *in vitro* incubation of blood samples with ethanol, higher concentrations of ethanol (86.8 mM) affected the deformability of neutrophils and monocytes.

Jacobi and colleagues investigated the effects of **gadolinium-based contrast agents** on the mechanical properties of lymphocytes [65]. Gadolinium-based contrast agents (GBCAs) are used in magnetic resonance imaging (MRI) to improve image quality. In the study, several GBCAs were tested and significant changes in the mechanical properties of leucocytes were measured by sDC.

Finally, an important area where sDC may find its usage is the assessment of blood cells during **cell therapies** and **cell product manufacturing**. One example is the purification process, which often relies on microfluidic methods. To avoid clogging of microfluidic channels, surfactant molecules are commonly added, with Pluronic F-68 being one of the most widely used. However, very little is known about its effect on the mechanical properties of the cells. Guzniczak and colleagues observed stiffening of Jurkat cells and red blood cells after 3 h incubation with 1 % Pluronic F-68 [67]. Pfister and colleagues studied the impact of loading superparamagnetic iron oxide **nanoparticles** (SPIONs) into the T cells used for cancer immunotherapy [72]. SPIONs

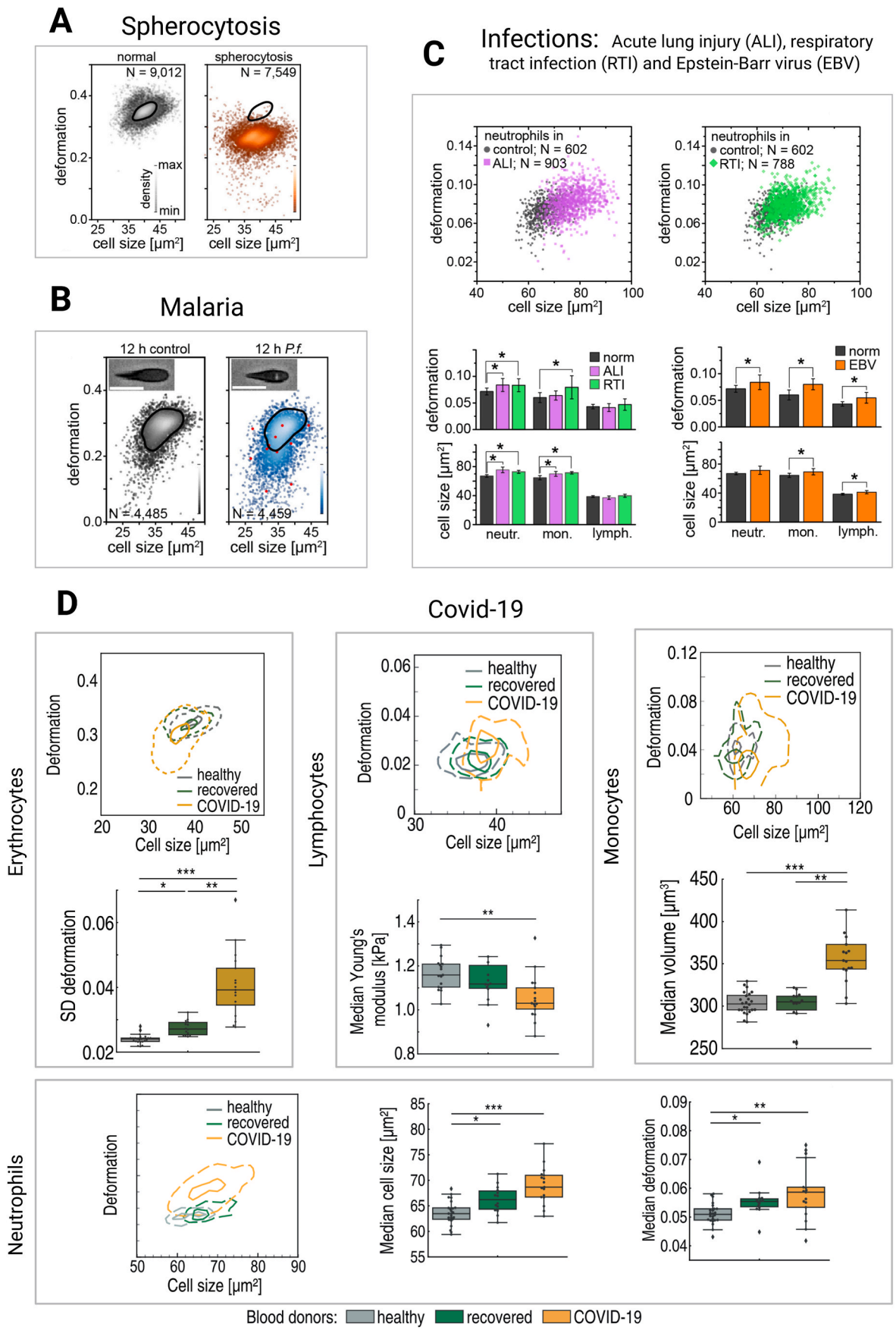

(caption on next page)

Fig. 5. Notable findings from studies using sDC on human blood samples for diagnostic applications. A-D) Comparison of cellular characteristics between patients and healthy donors. Each density plot is a representative result from a set of samples. A, B) Density plots of deformation versus cell size (cross-sectional area) for erythrocytes from A) spherocytosis patient (orange) and healthy donor (black) and B) control (black) and erythrocytes exposed to *Plasmodium falciparum* (blue) after 12 h incubation. C) Density plots of deformation versus cell size (cross-sectional area) of neutrophils from a patient with ALI (magenta) and RTI (green) compared to respective controls in black, mean and SD of cell size and deformation for neutrophils, monocytes and lymphocytes in ALI (magenta), RTI (green) and EBV (orange) patients compared to controls. D) Density plots showing the differences in cell size (cross-sectional area) and deformation between healthy donor, patient 4 months after COVID-19 infection and patient with COVID-19 in intensive care unit for erythrocytes, lymphocytes, monocytes and neutrophils and the mean or SD of the variables that differed most between the three groups tested for each cell type. (A–C) Adapted from Ref. [51] under the terms of the Creative Commons Attribution License (CC BY). D) Adapted from Ref. [62] under the terms of the Creative Commons Attribution License (CC BY-NC-ND). (For interpretation of the references to color in this figure legend, the reader is referred to the Web version of this article.)

can help guide T cells toward tumors, addressing infiltration issues and other difficulties that can limit their efficacy in solid tumor therapies. SPION loaded T cells showed no changes in their mechanical properties.

3.2. Tissue cells and cell lines

sDC also shows potential for detecting changes in the physiological state of tissue cells and adherent cell lines, although they require additional steps in sample preparation (Fig. 4B and C and D). For example, sDC may be particularly useful in solid tumor research, as cancer cells are known to adapt both biochemically and mechanically to changing external conditions during metastatic progression [91].

Assessment of tissue samples using sDC is still in its early stages. A notable example in this area is the study by Soteriou and colleagues who proposed the use of real-time fluorescent and deformability cytometry to characterize tumor biopsy samples during surgery (Fig. 6) [79]. Currently, histological characterization remains the standard method, but it is time-consuming, labor- and cost-intensive, and requires a trained expert. In turn, sDC combined with fluorescence detection was successfully used to differentiate subpopulations of cells from **mouse liver, colon and kidney tissue biopsies**. The samples were prepared using a tissue grinder, enabling enzyme-free mechanical cell dissociation. In addition, the research showed that this method can be used to assess the level of inflammation in tissues and to detect malignancy (Fig. 6) [79]. Conti et al. (2024) analyzed organoids derived from patients with colorectal cancer and found that LGR5 expression levels defined different mechanical phenotypes [78]. LGR5+ cells were stiffer, more adherent and slower moving, with nuclear YAP and high survival under mechanical stress, indicating mechanical stability. In contrast, LGR5 cells were softer, less adherent and faster, representing a more dynamic state. These differences suggest complementary roles in metastasis: LGR5 cells facilitate escape from the primary tumor and invasion, while LGR5+ cells support long-term metastatic growth.

The analysis of cell lines using sDC is more widespread. For example, Tavares and colleagues observed that, prior to acquiring malignant features, the **MCF10A breast cancer cells** initially became stiffer due to changes in actin fiber organization, which was surprising as cancerous cells are commonly more deformable than normal cells [83]. Using the same cell line, it was also established that expression of the RasV12 oncogene profoundly alters the shape dynamics and mechanics of mitotic cells, enhancing their ability to undergo error-free divisions in confined environments such as tumors [84]. The correlation between the mechanical properties of the extracellular matrix, and the stiffness of cancer cells and their invasive potential was demonstrated in a systematic comparison of cells from different cancers, including **breast**, **colorectal** and **pancreatic cancers** [85], exposed to different stiffnesses of their environment. Later, a correlation between the cells of different invasive potential and their stiffness was found even within one cell type, as Zemljič-Jokhadar and colleagues showed that a floating subpopulation of **MDA breast cancer cells** was softer than their adherent counterpart, even when grown in the same growth flask [86]. Bemmerlein et al. (2022) observed that different morphotypes of breast cancer cells correlated with the stiffness of the cells and their migratory potential in metastasis [82].

Differences between the cancer cells and their normal variants have also been found in other cancers, such as **osteosarcoma** [87]. sDC has also been employed in studies of cancer-associated cells. Increased stiffness was observed in **cancer-associated fibroblasts** from patients' **malignant prostate tissue** compared to non-malignant prostate tissue [77]. On the other hand, epithelial cells became softer when co-cultured with fibroblasts from malignant tissue. Similar mechanical adaptations of cells were also observed with cancer-associated fibroblasts from patients with **head and neck squamous cell carcinoma** [80].

Another area, where cell mechanics plays an important role is cell differentiation and adaptation to the extracellular matrix. For example, sDC has been used to quantify the differences in cell mechanics that

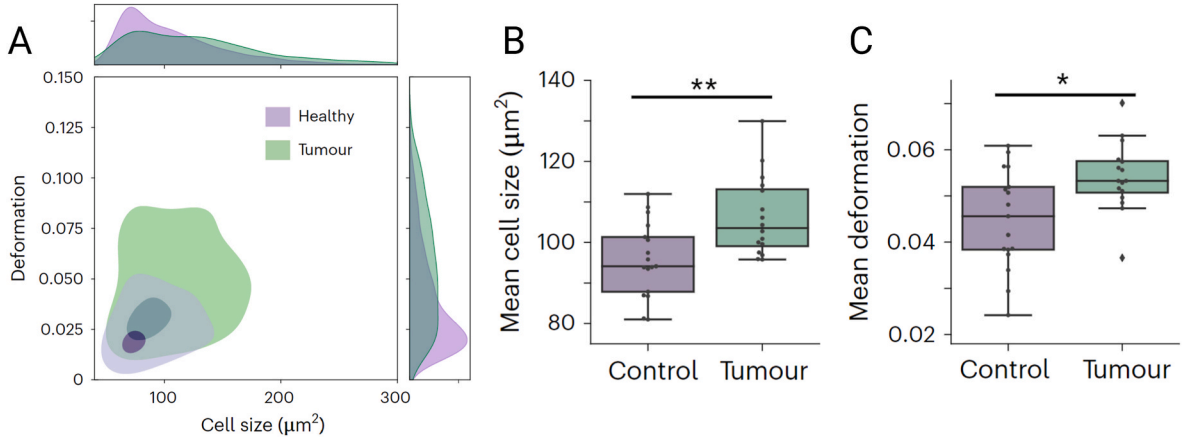

Fig. 6. Comparison of cells isolated from healthy and tumor mouse colon tissue. A) Kernel density estimate plots, with contours marking the 0.5 (light shade, outer contour) and 0.95 (dark shade, inner contour) levels. B) Mean cell size (cross-sectional area) and C) Mean deformation, two examples of features that were found to be significantly different between samples from tumor and healthy mouse colon. Adapted from Ref. [79] under the terms of the Creative Commons Attribution License (CC BY). (For interpretation of the references to color in this figure legend, the reader is referred to the Web version of this article.)

occur during the differentiation of **stem cells,** such as **cardiac progenitor cells** into cardiomyocytes [88]. Similarly, differences in mechanical properties have been found between bone marrow-derived **skeletal stem cells** with multipotent differentiation potential and three primary leukocyte lineages (lymphocytes, monocytes and granulocytes) as well as a human leukemic progenitor cell line [81].

4. Discussion: moving towards applications in clinical settings

Among the many published approaches for mechanical and morphological analysis of single cells, shear flow deformability cytometry stands out as the one having the most published applications. Its popularity can be attributed to several factors, including its high-throughput, high-resolution imaging of single cells, robust and simple operation, demonstrated use of whole blood samples, requirement of small sample volumes and inexpensive consumables. Furthermore, sDC has been successfully applied for analysis of many cell types in both health and disease. However, challenges remain before it can be established as a standard clinical tool.

Despite the widespread adoption of microfluidic devices in research laboratories, few have transitioned into clinical settings. Microfluidics has been used to study blood cells already in the early 2000s [92], and since then the research environment witnessed a rapid advance of various high-throughput microfluidic techniques for single cell analysis [29]. Nevertheless, the clinical application of microfluidic technology remained limited, with a notable exception in the detection of circulating tumor cells [93], and most recently with a novel sepsis test [94].

Recent review by Natu et al. [95] has analyzed trends in the medical adoption of microfluidic devices, noting a sharp increase in submissions for U.S. Food and Drug Administration (FDA) approval, particularly during the COVID-19 pandemic. However, only 1 % of these submissions involved De Novo Classification Requests, i.e., submissions for devices lacking a legally marketed predicate. This finding suggests that obtaining FDA or equivalent regulatory approval for novel microfluidic devices remains a complex process, imposing a considerable resource burden due to the extensive testing and specialized expertise required to demonstrate safety, accuracy, reliability, and robustness [96].

A significant challenge for the clinical adoption of DC is achieving manufacturing scalability of microfluidic chips, as the fabrication process must transition from polydimethylsiloxane (PDMS)-based soft lithography, commonly used in research, to a mass-producible, high-precision microfluidic device. PDMS is a soft, porous polymer that can expand under applied pressure, making it less suitable for high-throughput applications. Currently, few off-the-shelf thermoplastic chips (e.g., copolymer (COC), polymethylmethacrylate (PMMA), or polycarbonate (PC)) offer features as small as the narrow channel of sDC (20 μm). However, by leveraging high-precision molding techniques such as micro-injection molding and hot embossing, both the manufacturability and reliability of durable, biocompatible thermoplastic chips can, in principle, be achieved [97]. Equally important is the implementation of advanced bonding methods—including thermal fusion bonding, solvent-assisted bonding, and ultrasonic welding—to replace PDMS plasma bonding.

Additionally, sample manipulation (e.g., pumping) and readout processes will need adaptation to ensure high precision required for clinical applications; for example, even a minimal drift in the optical focus plane can significantly impact DC measurements. Implementing these modifications while maintaining device integrity is a costly and labor-intensive process, potentially posing a significant barrier for manufacturers.

Beyond the identification and investigation of potential mechanical biomarkers in research labs, deformability metrics will require extensive validation to establish their diagnostic utility, as regulatory bodies demand clear clinical benefits and robust evidence for approval. Standardizing protocols and data interpretation will be essential to meet these requirements. The inventors of sDC have made substantial efforts to promote transparency, publishing the basic design principles, releasing much of the analytical software under open-source licensing, and providing comprehensive documentation. Moreover, they established an open repository for deformability cytometry data, the Deformability Cytometry Open Repository (DCOR; https://dcor.mpl.mpg.de/) to facilitate transparent data exchange for re-analysis. Still, only a small number of datasets have been uploaded to this repository so far. Also, it remains uncertain whether future AI models developed for cell analysis and classification will follow this open-source approach. In addition, the AI models will have to adhere to the guidelines for adoption of AI in biomedicine that are currently under development [98].

A final challenge will be the integration of DC devices within clinical workflows. Routine clinical use will require compatibility with existing equipment and healthcare processes, including seamless data flow, while also necessitating additional training for clinicians and laboratory personnel. Adjustments in workflow and protocol may encounter logistical and administrative challenges and achieving cost efficiency will be a prerequisite for successful commercialization. A potential model for clinical adoption is the Cytovale Intellisep Sepsis Test, which made a significant effort to distill the complex results of a DC method into a simple 10-grade scale, the Intellisep Index (ISI), further divided into three bands (low, medium, and high probability of sepsis), making it readily applicable in clinical practice [94].

This review primarily focused on sDC; however, it should be noted that sDC shares many similarities with other DC methods, and advancements in one approach can readily benefit others. For example, all these methods will benefit from advancements in mass manufacturing of microfluidic chips, flow control integration, and innovations in image processing and AI-driven image analysis.

In conclusion, shear flow deformability cytometry (sDC) holds significant promise as one of the first microfluidic methods to be widely adopted for routine clinical diagnostics. Operating with a complexity comparable to current clinical cell counters and requiring only minimal blood volumes, sDC additionally offers novel mechanical parameters not accessible through existing methods. Furthermore, the development of sDC has been notably transparent, with much of the analytical software and acquired data openly available. It now falls to the research community to uphold this transparency, explore new mechanical biomarkers, and undertake the rigorous cross-laboratory validation that will encourage manufacturers to apply for the regulatory approvals and finally advance the method towards clinical adoption.

CRediT authorship contribution statement

Lija Fajdiga: Writing – review & editing, Writing – original draft, Visualization, Conceptualization. **Špela Zemljič:** Writing – review & editing, Writing – original draft, Conceptualization. **Tadej Kokalj:** Writing – review & editing, Writing – original draft, Supervision, Conceptualization. **Jure Derganc:** Writing – review & editing, Writing – original draft, Visualization, Supervision, Conceptualization.

Declaration of generative AI and AI-assisted technologies in the writing process

During the preparation of this work the author(s) used ChatGPT and InstaText in order to proof-read the manuscript. After using this tool/service, the author(s) reviewed and edited the content as needed and take(s) full responsibility for the content of the publication.

Declaration of competing interest

The authors declare that they have no known competing financial interests or personal relationships that could have appeared to influence the work reported in this paper.

Acknowledgements

This work was supported by the Slovenian Research and Innovation Agency, through grants P1-0055, P2-0132, J7-4493 and J2-50092.

Data availability

No data was used for the research described in the article.

References

[1] R. Green, S. Wachsmann-Hogiu, Development, history, and future of automated cell counters, Clin. Lab. Med. 35 (2015) 1–10, https://doi.org/10.1016/j.cll.2014.11.003.
[2] D.L. Jaye, R.A. Bray, H.M. Gebel, W.A.C. Harris, E.K. Waller, Translational applications of flow cytometry in clinical practice, J. Immunol. 188 (2012) 4715–4719, https://doi.org/10.4049/jimmunol.1290017.
[3] A. Bodaghi, N. Fattahi, A. Ramazani, Biomarkers: promising and valuable tools towards diagnosis, prognosis and treatment of Covid-19 and other diseases, Heliyon 9 (2023) e13323, https://doi.org/10.1016/j.heliyon.2023.e13323.
[4] N.R. Cook, Quantifying the added value of new biomarkers: how and how not, Diagn Progn. Res. 2 (2018), https://doi.org/10.1186/s41512-018-0037-2.
[5] D. Di Carlo, A mechanical biomarker of cell state in medicine, J. Lab. Autom. 17 (2012) 32–42, https://doi.org/10.1177/2211068211431630.
[6] M. Eroles, F. Rico, Advances in mechanical biomarkers, J. Mol. Recogn. 36 (2023), https://doi.org/10.1002/jmr.3022.
[7] M. Urbanska, J. Guck, Single-cell mechanics: structural determinants and functional relevance. https://doi.org/10.1146/annurev-biophys-030822, 2024.
[8] M. Chapman, V. Rajagopal, A. Stewart, D.J. Collins, Critical review of single-cell mechanotyping approaches for biomedical applications, Lab Chip 24 (2024) 3036–3063, https://doi.org/10.1039/d3lc00978e.
[9] J. Guck, E.R. Chilvers, Mechanics meets medicine, Sci. Transl. Med. 5 (2013), https://doi.org/10.1126/scitranslmed.3007731.
[10] L. Da Costa, L. Suner, J. Galimand, A. Bonnel, T. Pascreau, N. Couque, O. Fenneteau, N. Mohandas, Diagnostic tool for red blood cell membrane disorders: assessment of a new generation ektacytometer, Blood Cells Mol. Dis. 56 (2016) 9–22, https://doi.org/10.1016/j.bcmd.2015.09.001.
[11] E.M. Darling, D. Di Carlo, High-throughput assessment of cellular mechanical properties, Annu. Rev. Biomed. Eng. 17 (2015) 35–62, https://doi.org/10.1146/annurev-bioeng-071114-040545.
[12] T.W. Murphy, Q. Zhang, L.B. Naler, S. Ma, C. Lu, Recent advances in the use of microfluidic technologies for single cell analysis, Analyst 143 (2018) 60–80, https://doi.org/10.1039/c7an01346a.
[13] L. An, F. Ji, E. Zhao, Y. Liu, Y. Liu, Measuring cell deformation by microfluidics, Front. Bioeng. Biotechnol. 11 (2023), https://doi.org/10.3389/fbioe.2023.1214544.
[14] H. Kim, A. Zhbanov, S. Yang, Microfluidic systems for blood and blood cell characterization, Biosensors 13 (2023), https://doi.org/10.3390/bios13010013.
[15] M.J. Rosenbluth, W.A. Lam, D.A. Fletcher, Analyzing cell mechanics in hematologic diseases with microfluidic biophysical flow cytometry, Lab Chip 8 (2008) 1062–1070, https://doi.org/10.1039/b802931h.
[16] J. Chen, Y. Zheng, Q. Tan, E. Shojaei-Baghini, Y.L. Zhang, J. Li, P. Prasad, L. You, X. Y. Wu, Y. Sun, Classification of cell types using a microfluidic device for mechanical and electrical measurement on single cells, Lab Chip 11 (2011) 3174–3181, https://doi.org/10.1039/c1lc20473d.
[17] H. Bow, I.V. Pivkin, M. Diez-Silva, S.J. Goldfless, M. Dao, J.C. Niles, S. Suresh, J. Han, A microfabricated deformability-based flow cytometer with application to malaria, in: Lab Chip, Royal Society of Chemistry, 2011, pp. 1065–1073, https://doi.org/10.1039/c0lc00472c.
[18] M. Abkarian, M. Faivre, H.A. Stone, High-speed microfluidic differential manometer for cellular-scale hydrodynamics. www.pnas.orgcgidoi10.1073pnas.0507171102, 2006.
[19] D.R. Gossett, H.T.K. Tse, S.A. Lee, Y. Ying, A.G. Lindgren, O.O. Yang, J. Rao, T. Clark, D. Di Carlo, Hydrodynamic stretching of single cells for large population mechanical phenotyping, Proc. Natl. Acad. Sci. USA 109 (2012) 7630–7635, https://doi.org/10.1073/pnas.1200107109/-/DCSupplemental.
[20] F.J. Armistead, J. Gala De Pablo, H. Gadêlha, S.A. Peyman, S.D. Evans, Cells under stress: an inertial-shear microfluidic determination of cell behavior, Biophys. J. 116 (2019) 1127–1135, https://doi.org/10.1016/j.bpj.2019.01.034.
[21] V. Faustino, R.O. Rodrigues, D. Pinho, E. Costa, A. Santos-Silva, V. Miranda, J. S. Amaral, R. Lima, A microfluidic deformability assessment of pathological red blood cells flowing in a hyperbolic converging microchannel, Micromachines 10 (2019), https://doi.org/10.3390/mi10100645.
[22] R. Reale, A. De Ninno, T. Nepi, P. Bisegna, F. Caselli, Extensional-flow impedance cytometer for contactless and optics-free erythrocyte deformability analysis, IEEE Trans. Biomed. Eng. 70 (2023) 565–572, https://doi.org/10.1109/TBME.2022.3197214.
[23] C. Petchakup, H. Yang, L. Gong, L. He, H.M. Tay, R. Dalan, A.J. Chung, K.H.H. Li, H.W. Hou, Microfluidic impedance-deformability cytometry for label-free single neutrophil mechanophenotyping, Small 18 (2022), https://doi.org/10.1002/smll.202104822.
[24] O. Otto, P. Rosendahl, A. Mietke, S. Golfier, C. Herold, D. Klaue, S. Girardo, S. Pagliara, A. Ekpenyong, A. Jacobi, M. Wobus, N. Töpfner, U.F. Keyser, J. Mansfeld, E. Fischer-Friedrich, J. Guck, Real-time deformability cytometry: on-the-fly cell mechanical phenotyping, Nat. Methods 12 (2015) 199–202, https://doi.org/10.1038/nmeth.3281.
[25] M. Asghari, S. Duclos Ivetich, M.K. Aslan, M. Aramesh, O. Melkonyan, Y. Meng, R. Xu, M. Colombo, T. Weiss, S. Balabanov, S. Stavrakis, A.J. Demello, Real-time viscoelastic deformability cytometry: high-throughput mechanical phenotyping of liquid and solid biopsies. https://www.science.org, 2024.
[26] Y. Belotti, S. Tolomeo, M.J. Conneely, T. Huang, S.J. McKenna, G. Nabi, D. McGloin, High-throughput, time-resolved mechanical phenotyping of prostate cancer cells, Sci. Rep. 9 (2019), https://doi.org/10.1038/s41598-019-42008-0.
[27] D. Dannhauser, M.I. Maremonti, V. Panzetta, D. Rossi, P.A. Netti, F. Causa, Mechanical phenotyping of breast cell lines by in-flow deformation-dependent dynamics under tuneable compressive forces, Lab Chip 20 (2020) 4611–4622, https://doi.org/10.1039/d0lc00911c.
[28] M. Doan, I. Vorobjev, P. Rees, A. Filby, O. Wolkenhauer, A.E. Goldfeld, J. Lieberman, N. Barteneva, A.E. Carpenter, H. Hennig, Diagnostic potential of imaging flow cytometry, Trends Biotechnol. 36 (2018) 649–652, https://doi.org/10.1016/j.tibtech.2017.12.008.
[29] S. Stavrakis, G. Holzner, J. Choo, A. deMello, High-throughput microfluidic imaging flow cytometry, Curr. Opin. Biotechnol. 55 (2019) 36–43, https://doi.org/10.1016/j.copbio.2018.08.002.
[30] Y. Chen, K. Guo, L. Jiang, S. Zhu, Z. Ni, N. Xiang, Microfluidic deformability cytometry: a review, Talanta 251 (2022), https://doi.org/10.1016/j.talanta.2022.123815.
[31] H. Chen, J. Guo, F. Bian, Y. Zhao, Microfluidic technologies for cell deformability cytometry, Smart Med. 1 (2022), https://doi.org/10.1002/smmd.20220001.
[32] M. Urbanska, H.E. Muñoz, J. Shaw Bagnall, O. Otto, S.R. Manalis, D. Di Carlo, J. Guck, A comparison of microfluidic methods for high-throughput cell deformability measurements, Nat. Methods 17 (2020) 587–593, https://doi.org/10.1038/s41592-020-0818-8.
[33] S. Zhou, B. Chen, E.S. Fu, H. Yan, Computer vision meets microfluidics: a label-free method for high-throughput cell analysis, Microsyst. Nanoeng. 9 (2023), https://doi.org/10.1038/s41378-023-00562-8.
[34] A. Mietke, O. Otto, S. Girardo, P. Rosendahl, A. Taubenberger, S. Golfier, E. Ulbricht, S. Aland, J. Guck, E. Fischer-Friedrich, Extracting cell stiffness from real-time deformability cytometry: theory and experiment, Biophys. J. 109 (2015) 2023–2036, https://doi.org/10.1016/j.bpj.2015.09.006.
[35] P. Rosendahl, K. Plak, A. Jacobi, M. Kraeter, N. Toepfner, O. Otto, C. Herold, M. Winzi, M. Herbig, Y. Ge, S. Girardo, K. Wagner, B. Baum, J. Guck, Real-time fluorescence and deformability cytometry, Nat. Methods 15 (2018) 355–358, https://doi.org/10.1038/nmeth.4639.
[36] M. Herbig, K. Tessmer, M. Nötzel, A.A. Nawaz, T. Santos-Ferreira, O. Borsch, S. J. Gasparini, J. Guck, M. Ader, Label-free imaging flow cytometry for analysis and sorting of enzymatically dissociated tissues, Sci. Rep. 12 (2022), https://doi.org/10.1038/s41598-022-05007-2.
[37] A.A. Nawaz, M. Urbanska, M. Herbig, M. Nötzel, M. Kräter, P. Rosendahl, C. Herold, N. Toepfner, M. Kubánková, R. Goswami, S. Abuhattum, F. Reichel, P. Müller, A. Taubenberger, S. Girardo, A. Jacobi, J. Guck, Intelligent image-based deformation-assisted cell sorting with molecular specificity, Nat. Methods 17 (2020) 595–599, https://doi.org/10.1038/s41592-020-0831-y.
[38] E. Shojaei-Baghini, Y. Zheng, M.A.S. Jewett, W.B. Geddie, Y. Sun, Mechanical characterization of benign and malignant urothelial cells from voided urine, Appl. Phys. Lett. 102 (2013), https://doi.org/10.1063/1.4798495.
[39] J. Kim, S. Han, A. Lei, M. Miyano, J. Bloom, V. Srivastava, M.R. Stampfer, Z. J. Gartner, M.A. Labarge, L.L. Sohn, Characterizing cellular mechanical phenotypes with mechano-node-pore sensing, Microsyst. Nanoeng. 4 (2018), https://doi.org/10.1038/MICRONANO.2017.91.
[40] R.E. Waugh, E. Lomakina, A. Amitrano, M. Kim, Activation effects on the physical characteristics of T lymphocytes, Front. Bioeng. Biotechnol. 11 (2023), https://doi.org/10.3389/fbioe.2023.1175570.
[41] A.D. Stephens, E.J. Banigan, S.A. Adam, R.D. Goldman, J.F. Marko, Chromatin and lamin a determine two different mechanical response regimes of the cell nucleus, Mol. Biol. Cell 28 (2017) 1984–1996, https://doi.org/10.1091/mbc.E16-09-0653.
[42] Š.Z. Jokhadar, J. Derganc, Structural rearrangements in CHO cells after disruption of individual cytoskeletal elements and plasma membrane, Cell Biochem. Biophys. 71 (2015) 1605–1613, https://doi.org/10.1007/s12013-014-0383-9.
[43] P.H. Wu, D.R. Ben Aroush, A. Asnacios, W.C. Chen, M.E. Dokukin, B.L. Doss, P. Durand-Smet, A. Ekpenyong, J. Guck, N.V. Guz, P.A. Janmey, J.S.H. Lee, N. M. Moore, A. Ott, Y.C. Poh, R. Ros, M. Sander, I. Sokolov, J.R. Staunton, N. Wang, G. Whyte, D. Wirtz, A comparison of methods to assess cell mechanical properties, Nat. Methods 15 (2018) 491–498, https://doi.org/10.1038/s41592-018-0015-1.
[44] K. Lei, A. Kurum, M. Kaynak, et al., Cancer-cell stiffening via cholesterol depletion enhances adoptive T-cell immunotherapy, Nat. Biomed. Eng. 5 (2021) 1411–1425. https://doi.org/10.1038/s41551-021-00826-6.
[45] H. Mziaut, B. Mulligan, P. Hoboth, O. Otto, A. Ivanova, M. Herbig, D. Schumann, T. Hildebrandt, J. Dehghany, A. Sönmez, C. Münster, M. Meyer-Hermann, J. Guck, Y. Kalaidzidis, M. Solimena, The F-actin modifier villin regulates insulin granule dynamics and exocytosis downstream of islet cell autoantigen 512, Mol. Metabol. 5 (2016) 656–668, https://doi.org/10.1016/j.molmet.2016.05.015.
[46] S. Golfier, P. Rosendahl, A. Mietke, M. Herbig, J. Guck, O. Otto, High-throughput cell mechanical phenotyping for label-free titration assays of cytoskeletal modifications, Cytoskeleton 74 (2017) 283–296, https://doi.org/10.1002/cm.21369.
[47] C.J. Chan, A.E. Ekpenyong, S. Golfier, W. Li, K.J. Chalut, O. Otto, J. Elgeti, J. Guck, F. Lautenschläger, Myosin II activity softens cells in suspension, Biophys. J. 108 (2015) 1856–1869, https://doi.org/10.1016/j.bpj.2015.03.009.

[48] J.R. Lange, J. Steinwachs, T. Kolb, L.A. Lautscham, I. Harder, G. Whyte, B. Fabry, Microconstriction arrays for high-throughput quantitative measurements of cell mechanical properties, Biophys. J. 109 (2015) 26–34, https://doi.org/10.1016/j.bpj.2015.05.029.
[49] M. Masaeli, D. Gupta, S. O'Byrne, H.T.K. Tse, D.R. Gossett, P. Tseng, A.S. Utada, H. J. Jung, S. Young, A.T. Clark, D. Di Carlo, Multiparameter mechanical and morphometric screening of cells, Sci. Rep. 6 (2016), https://doi.org/10.1038/srep37863.
[50] L.D. Wittwer, F. Reichel, P. Müller, J. Guck, S. Aland, A new hyperelastic lookup table for RT-DC, Soft Matter 19 (2023) 2064–2073, https://doi.org/10.1039/d2sm01418a.
[51] N. Toepfner, C. Herold, O. Otto, P. Rosendahl, A. Jacobi, M. Krä Ter, J. Stä Chele, L. Menschner, M. Herbig, L. Ciuffreda, L. Ranford-Cartwright, M. Grzybek, N. Tregay, M. Suttorp, M. Bornhä User, E.R. Chilvers, R. Berner, J. Guck, Detection of human disease conditions by single-cell morpho-rheological phenotyping of blood, Elife 7 (2018), https://doi.org/10.7554/eLife.29213.001.
[52] H.T.K. Tse, D.R. Gossett, Y.S. Moon, M. Masaeli, M. Sohsman, Y. Ying, K. Mislick, R.P. Adams, J. Rao, D. Di Carlo, B I O E N G I N E E R I N G, Quantitative diagnosis of malignant pleural effusions by single-cell mechanophenotyping. https://doi.org/10.1126/scitranslmed.3006559, 2013.
[53] Müller Paul, others, Shape-Out version 2.X.X: analysis software for real-time deformability cytometry [Software], https://github.com/ZELLMECHANIK-DRESDEN/ShapeOut2, 2019.
[54] M. Herbig, A. Mietke, P. Müller, O. Otto, Statistics for real-time deformability cytometry: clustering, dimensionality reduction, and significance testing, Biomicrofluidics 12 (2018), https://doi.org/10.1063/1.5027197.
[55] M. Mokbel, D. Mokbel, A. Mietke, N. Träber, S. Girardo, O. Otto, J. Guck, S. Aland, Numerical simulation of real-time deformability cytometry to extract cell mechanical properties, ACS Biomater. Sci. Eng. 3 (2017) 2962–2973, https://doi.org/10.1021/acsbiomaterials.6b00558.
[56] Y. Ge, P. Rosendahl, C. Duran, N. Topfner, S. Ciucci, J. Guck, C.V. Cannistraci, Cell mechanics based computational classification of red blood cells via machine intelligence applied to morpho-rheological markers, IEEE ACM Trans. Comput. Biol. Bioinf 18 (2021) 1405–1415, https://doi.org/10.1109/TCBB.2019.2945762.
[57] M. Kräter, S. Abuhattum, D. Soteriou, A. Jacobi, T. Krüger, J. Guck, M. Herbig, AIDeveloper: deep learning image classification in life science and beyond, Adv. Sci. 8 (2021), https://doi.org/10.1002/advs.202003743.
[58] M. Herbig, A. Jacobi, M. Wobus, H. Weidner, A. Mies, M. Kräter, O. Otto, C. Thiede, M.T. Weickert, K.S. Götze, M. Rauner, L.C. Hofbauer, M. Bornhäuser, J. Guck, M. Ader, U. Platzbecker, E. Balaian, Machine learning assisted real-time deformability cytometry of CD34+ cells allows to identify patients with myelodysplastic syndromes, Sci. Rep. 12 (2022), https://doi.org/10.1038/s41598-022-04939-z.
[59] C. Zhang, M. Herbig, Y. Zhou, M. Nishikawa, M. Shifat-E-Rabbi, H. Kanno, R. Yang, Y. Ibayashi, T.H. Xiao, G.K. Rohde, M. Sato, S. Kodera, M. Daimon, Y. Yatomi, K. Goda, Real-time intelligent classification of COVID-19 and thrombosis via massive image-based analysis of platelet aggregates, Cytometry A 103 (2023) 492–499, https://doi.org/10.1002/cyto.a.24721.
[60] M. Kräter, S. Abuhattum, D. Soteriou, A. Jacobi, T. Krüger, J. Guck, M. Herbig, AIDeveloper: deep learning image classification in life science and beyond, Adv. Sci. 8 (2021), https://doi.org/10.1002/advs.202003743.
[61] M. Herbig, A. Jacobi, M. Wobus, H. Weidner, A. Mies, M. Kräter, O. Otto, C. Thiede, M.T. Weickert, K.S. Götze, M. Rauner, L.C. Hofbauer, M. Bornhäuser, J. Guck, M. Ader, U. Platzbecker, E. Balaian, Machine learning assisted real-time deformability cytometry of CD34+ cells allows to identify patients with myelodysplastic syndromes, Sci. Rep. 12 (2022), https://doi.org/10.1038/s41598-022-04939-z.
[62] M. Kubánková, B. Hohberger, J. Hoffmanns, J. Fürst, M. Herrmann, J. Guck, M. Kräter, Physical phenotype of blood cells is altered in COVID-19, Biophys. J. 120 (2021) 2838–2847, https://doi.org/10.1016/j.bpj.2021.05.025.
[63] J. Eder, L. Schumm, J.P. Armann, M.A. Puhan, F. Beuschlein, C. Kirschbaum, R. Berner, N. Toepfner, Increased red blood cell deformation in children and adolescents after SARS-CoV-2 infection, Sci. Rep. 13 (2023), https://doi.org/10.1038/s41598-023-35692-6.
[64] P. Shalchi-Amirkhiz, T. Bensch, U. Proschmann, A.K. Stock, T. Ziemssen, K. Akgün, Pilot study on the influence of acute alcohol exposure on biophysical parameters of leukocytes, Front. Mol. Biosci. 10 (2023), https://doi.org/10.3389/fmolb.2023.1243155.
[65] A. Jacobi, A.A. de Schellenberger, Y.O. Uca, M. Herbig, J. Guck, I. Sack, Real-time deformability cytometry detects leukocyte stiffening after gadolinium-based contrast agent exposure, Investig. Radiol. 56 (2021) 837–844, https://doi.org/10.1097/RLI.0000000000000794.
[66] A. Walther, A. Mackens-Kiani, J. Eder, M. Herbig, C. Herold, C. Kirschbaum, J. Guck, L.D. Wittwer, K. Beesdo-Baum, M. Kräter, Depressive disorders are associated with increased peripheral blood cell deformability: a cross-sectional case-control study (Mood-Morph), Transl. Psychiatry 12 (2022), https://doi.org/10.1038/s41398-022-01911-3.
[67] E. Guzniczak, M. Jimenez, M. Irwin, O. Otto, N. Willoughby, H. Bridle, Impact of poloxamer 188 (Pluronic F-68) additive on cell mechanical properties, quantification by real-time deformability cytometry, Biomicrofluidics 12 (2018), https://doi.org/10.1063/1.5040316.
[68] M. Koch, K.E. Wright, O. Otto, M. Herbig, N.D. Salinas, N.H. Tolia, T.J. Satchwell, J. Guck, N.J. Brooks, J. Baum, Plasmodium falciparum erythrocyte-binding antigen 175 triggers a biophysical change in the red blood cell that facilitates invasion, Proc. Natl. Acad. Sci. U. S. A. 114 (2017) 4225–4230, https://doi.org/10.1073/pnas.1620843114.
[69] C. Zaninetti, L. Sachs, R. Palankar, Role of platelet cytoskeleton in platelet biomechanics: current and emerging methodologies and their potential relevance for the investigation of inherited platelet disorders, Hämostaseologie 40 (2020) 337–347, https://doi.org/10.1055/a-1175-6783.
[70] L. Sachs, J. Wesche, L. Lenkeit, A. Greinacher, M. Bender, O. Otto, R. Palankar, Ex vivo anticoagulants affect human blood platelet biomechanics with implications for high-throughput functional mechanophenotyping, Commun. Biol. 5 (2022), https://doi.org/10.1038/s42003-021-02982-6.
[71] K. Aurich, J. Wesche, M. Ulbricht, O. Otto, A. Greinacher, R. Palankar, Divalent magnesium restores cytoskeletal storage lesions in cold-stored platelet concentrates, Sci. Rep. 12 (2022), https://doi.org/10.1038/s41598-022-10231-x.
[72] F. Pfister, J. Dörrie, N. Schaft, V. Buchele, H. Unterweger, L.R. Carnell, P. Schreier, R. Stein, M. Kubánková, J. Guck, H. Hackstein, C. Alexiou, C. Janko, Human T cells loaded with superparamagnetic iron oxide nanoparticles retain antigen-specific TCR functionality, Front. Immunol. 14 (2023), https://doi.org/10.3389/fimmu.2023.1223695.
[73] K.A.M. Ullrich, J. Derdau, C. Baltes, A. Battistella, G. Rosso, S. Uderhardt, L. Lou Schulze, L.J. Liu, M. Dedden, M. Spocinska, L. Kainka, M. Kubánková, T.M. Müller, N.M. Schmidt, E. Becker, O. Ben Brahim, I. Atreya, S. Finotto, I. Prots, S. Wirtz, B. Weigmann, R. López-Posadas, R. Atreya, A.B. Ekici, F. Lautenschläger, J. Guck, M.F. Neurath, S. Zundler, IL-3 receptor signalling suppresses chronic intestinal inflammation by controlling mechanobiology and tissue egress of regulatory T cells, Gut 72 (2023) 2081–2094, https://doi.org/10.1136/gutjnl-2023-329818.
[74] J.J. Lühr, N. Alex, L. Amon, M. Kräter, M. Kubánková, E. Sezgin, C.H.K. Lehmann, L. Heger, G.F. Heidkamp, A.S. Smith, V. Zaburdaev, R.A. Böckmann, I. Levental, M. L. Dustin, C. Eggeling, J. Guck, D. Dudziak, Maturation of monocyte-derived DCs leads to increased cellular stiffness, higher membrane fluidity, and changed lipid composition, Front. Immunol. 11 (2020), https://doi.org/10.3389/fimmu.2020.590121.
[75] M. Sampietro, V. Cassina, D. Salerno, F. Barbaglio, E. Buglione, C.A. Marrano, R. Campanile, L. Scarfò, D. Biedenweg, B. Fregin, M. Zamai, A. Díaz Torres, V. Labrador Cantarero, P. Ghia, O. Otto, F. Mantegazza, V.R. Caiolfa, C. Scielzo, The nanomechanical properties of CLL cells are linked to the actin cytoskeleton and are a potential target of BTK inhibitors, Hemasphere 7 (2023) E931, https://doi.org/10.1097/HS9.0000000000000931.
[76] A.E. Matei, M. Kubánková, L. Xu, A.H. Györfi, E. Boxberger, D. Soteriou, M. Papava, J. Prater, X. Hong, C. Bergmann, M. Kräter, G. Schett, J. Guck, J.H. W. Distler, Identification of a distinct monocyte-driven signature in systemic sclerosis using biophysical phenotyping of circulating immune cells, Arthritis Rheumatol. 75 (2023) 768–781, https://doi.org/10.1002/art.42394.
[77] A. Jaeschke, A. Jacobi, M.G. Lawrence, G.P. Risbridger, M. Frydenberg, E. D. Williams, I. Vela, D.W. Hutmacher, L.J. Bray, A. Taubenberger, Cancer-associated fibroblasts of the prostate promote a compliant and more invasive phenotype in benign prostate epithelial cells, Mater Today Bio. 8 (2020), https://doi.org/10.1016/j.mtbio.2020.100073.
[78] S. Conti, V. Venturini, A. Cañellas-Socias, C. Cortina, J.F. Abenza, C. Stephan-Otto Attolini, E. Middendorp Guerra, C.K. Xu, J.H. Li, L. Rossetti, G. Stassi, P. Roca-Cusachs, A. Diz-Muñoz, V. Ruprecht, J. Guck, E. Batlle, A. Labernadie, X. Trepat, Membrane to cortex attachment determines different mechanical phenotypes in LGR5+ and LGR5- colorectal cancer cells, Nat. Commun. 15 (2024), https://doi.org/10.1038/s41467-024-47227-2.
[79] D. Soteriou, M. Kubánková, C. Schweitzer, R. López-Posadas, R. Pradhan, O. M. Thoma, A.H. Györfi, A.E. Matei, M. Waldner, J.H.W. Distler, S. Scheuermann, J. Langejürgen, M. Eckstein, R. Schneider-Stock, R. Atreya, M.F. Neurath, A. Hartmann, J. Guck, Rapid single-cell physical phenotyping of mechanically dissociated tissue biopsies, Nat. Biomed. Eng. 7 (2023) 1392–1403, https://doi.org/10.1038/s41551-023-01015-3.
[80] B. Peltanová, H.H. Polanská, M. Raudenská, J. Balvan, J. Navrátil, T. Vičar, J. Gumulec, B. Čechová, M. Kräter, J. Guck, D. Kalfeřt, M. Grega, J. Plzák, J. Betka, M. Masařík, mRNA subtype of cancer-associated fibroblasts significantly affects key characteristics of head and neck cancer cells, Cancers 14 (2022), https://doi.org/10.3390/cancers14092286.
[81] M. Xavier, P. Rosendahl, M. Herbig, M. Kräter, D. Spencer, M. Bornhäuser, R.O. C. Oreffo, H. Morgan, J. Guck, O. Otto, Mechanical phenotyping of primary human skeletal stem cells in heterogeneous populations by real-time deformability cytometry, Integr. Biol. 8 (2016) 616–623, https://doi.org/10.1039/c5ib00304k.
[82] L. Bemmerlein, I.A. Deniz, J. Karbanová, A. Jacobi, S. Drukewitz, T. Link, A. Göbel, L. Sevenich, A.V. Taubenberger, P. Wimberger, J.D. Kuhlmann, D. Corbeil, Decoding single cell morphology in osteotropic breast cancer cells for dissecting their migratory, Mole. Biophys. Heterogeneity (2022), https://doi.org/10.3390/cancers.
[83] S. Tavares, A.F. Vieira, A.V. Taubenberger, M. Araújo, N.P. Martins, C. Brás-Pereira, A. Polónia, M. Herbig, C. Barreto, O. Otto, J. Cardoso, J.B. Pereira-Leal, J. Guck, J. Paredes, F. Janody, Actin stress fiber organization promotes cell stiffening and proliferation of pre-invasive breast cancer cells, Nat. Commun. 8 (2017), https://doi.org/10.1038/ncomms15237.
[84] H.K. Matthews, S. Ganguli, K. Plak, A.V. Taubenberger, Z. Win, M. Williamson, M. Piel, J. Guck, B. Baum, Oncogenic signaling alters cell shape and mechanics to facilitate cell division under confinement, Dev. Cell 52 (2020) 563–573.e3, https://doi.org/10.1016/j.devcel.2020.01.004.
[85] L. Wullkopf, A.K.V. West, N. Leijnse, T.R. Cox, C.D. Madsen, L.B. Oddershede, J. T. Erler, Cancer cells' ability to mechanically adjust to extracellular matrix stiffness correlates with their invasive potential, Mol. Biol. Cell 29 (2018) 2378–2385, https://doi.org/10.1091/mbc.E18-05-0319.
[86] Š. Zemljič-Jokhadar, G. Kokot, M. Pavlin, J. Derganc, Adhesion and stiffness of detached breast cancer cells in vitro: Co-treatment with metformin and 2-deoxy-D-

glucose induces changes related to increased metastatic potential, Biology 10 (2021), https://doi.org/10.3390/biology10090873.
[87] C.N. Holenstein, A. Horvath, B. Schär, A.D. Schoenenberger, M. Bollhalder, N. Goedecke, G. Bartalena, O. Otto, M. Herbig, J. Guck, D.A. Müller, J.G. Snedeker, U. Silvan, The relationship between metastatic potential and in vitro mechanical properties of osteosarcoma cells, Mol. Biol. Cell 30 (2019) 887–898, https://doi.org/10.1091/mbc.E18-08-0545.
[88] R.H. Pires, T.H. Dau, E. Manu, N. Shree, O. Otto, Switching in the expression pattern of actin isoforms marks the onset of contractility and distinct mechanodynamic behavior during cardiomyocyte differentiation, Phys. Rep. 10 (2022), https://doi.org/10.14814/phy2.15171.
[89] K.R. Bashant, A. Vassallo, C. Herold, R. Berner, L. Menschner, J. Subburayalu, M. J. Kaplan, C. Summers, J. Guck, E.R. Chilvers, N. Toepfner, Real-time deformability cytometry reveals sequential contraction and expansion during neutrophil priming, J. Leukoc. Biol. 105 (2019) 1143–1153, https://doi.org/10.1002/JLB.MA0718-295RR.
[90] F. Reichel, M. Kräter, K. Peikert, H. Glaß, P. Rosendahl, M. Herbig, A. Rivera Prieto, A. Kihm, G. Bosman, L. Kaestner, A. Hermann, J. Guck, Changes in blood cell deformability in chorea-acanthocytosis and effects of treatment with dasatinib or lithium, Front. Physiol. 13 (2022), https://doi.org/10.3389/fphys.2022.852946.
[91] Q.S. Li, G.Y.H. Lee, C.N. Ong, C.T. Lim, AFM indentation study of breast cancer cells, Biochem. Biophys. Res. Commun. 374 (2008) 609–613, https://doi.org/10.1016/j.bbrc.2008.07.078.
[92] S.C. Gifford, M.G. Frank, J. Derganc, C. Gabel, R.H. Austin, T. Yoshida, M. W. Bitensky, Parallel microchannel-based measurements of individual erythrocyte areas and volumes, Biophys. J. 84 (2003) 623–633.
[93] T.A. Burinaru, M. Avram, A. Avram, C. Marculescu, B. Tîncu, V. Tucureanu, A. Matei, M. Militaru, Detection of circulating tumor cells using microfluidics, ACS Comb. Sci. 20 (2018) 107–126, https://doi.org/10.1021/acscombsci.7b00146.
[94] H.R. O'Neal, R. Sheybani, D.R. Janz, R. Scoggins, T. Jagneaux, J.E. Walker, D. J. Henning, E. Rosenman, S.A. Mahler, H. Regunath, C.S. Sampson, D.C. Files, R. D. Fremont, M.J. Noto, E.E. Schneider, W.R. Shealey, M.S. Berlinger, T.C. Carver, M.K. Walker, N.A. Ledeboer, A.M. Shah, H.T.K. Tse, D. Dicarlo, T.W. Rice, C. B. Thomas, Validation of a novel, rapid sepsis diagnostic for emergency department use, Crit Care Explor 6 (2024) E1026, https://doi.org/10.1097/CCE.0000000000001026.
[95] R. Natu, L. Herbertson, G. Sena, K. Strachan, S. Guha, A systematic analysis of recent technology trends of microfluidic medical devices in the United States, Micromachines 14 (2023), https://doi.org/10.3390/mi14071293.
[96] M. Aboy, C. Crespo, A. Stern, Beyond the 510(k): the regulation of novel moderate-risk medical devices, intellectual property considerations, and innovation incentives in the FDA's De Novo pathway, NPJ Digit Med. 7 (2024), https://doi.org/10.1038/s41746-024-01021-y.
[97] S.M. Scott, Z. Ali, Fabrication methods for microfluidic devices: an overview, Micromachines 12 (2021), https://doi.org/10.3390/mi12030319.
[98] H.J. Warraich, T. Tazbaz, R.M. Califf, FDA perspective on the regulation of artificial intelligence in health care and biomedicine, JAMA (2024), https://doi.org/10.1001/jama.2024.21451.

GLOSSARY:

AFM –: atomic force microscopy
ALI –: acute lung injury
ALL -: acute lymphoblastic leukemia
AML -: acute myeloid leukemia
BTK -: Bruton's tyrosine kinase
CAFs –: cancer-associated fibroblasts
CBC -: complete blood count
cDC -: constriction-based deformability cytometry
CLL -: chronic lymphocytic leukemia
DC –: deformability cytometry
DCOR -: Deformability Cytometry Open Repository
DNN -: deep neural network
EBV -: Epstein-Barr virus
FDA -: U.S. Food and Drug Administration
GBCA -: gadolinium-based contrast agents
IL-3 -: interleukin-3
MC -: Methylcellulose
MDS -: myelodysplastic syndrome
moDC -: monocyte-derived dendritic cells
MRI -: magnetic resonance imaging
NK cells –: natural killer cells
PBMC -: peripheral blood mononuclear cell
PDMS –: polydimethylsiloxane
PHD2 -: prolyl hydroxylase domain protein 2
RBC –: red blood cells
RT-DC –: real-time deformability cytometry
RT-FDC –: real-time fluorescence deformability cytometry
RTI –: respiratory tract infection
sDC –: shear flow deformability cytometry
SPION -: superparamagnetic iron oxide nanoparticles
vDC -: viscoelastic deformability cytometry
WBC –: white blood cells
xDC -: extensional flow deformability cytometry

Lija Fajdiga received her bachelor's and master's degrees in biotechnology at the Biotechnical Faculty of the University of Ljubljana. She is currently a Ph.D. student under the supervision of Prof. Jure Derganc at the Institute of Biophysics, Faculty of Medicine, University of Ljubljana. Her current research focuses on understanding the mechanical properties of lymphocytes using various techniques from cell biology and immunology to biophysical measurements of cell mechanics and microfluidics.

Špela Zemljič is a senior researcher at the Institute of Biophysics at the Faculty of Medicine in Ljubljana. She obtained her Masters in Biology and her Ph.D. in Biotechnological sciences from University of Ljubljana. Her research interest is mainly focused on the mechanical properties of human cells.

Tadej Kokalj is a senior researcher at Institute of Metals and Technology, Laboratory for surface analysis. He obtained his Masters in Physics and Ph.D. in Mechanical Engineering at University of Ljubljana. He pursued his postdoctoral training in field of materials and later in microfluidics and biosensors at KU Leuven and in bio-microfluidics as a Fulbright scholar at UC Berkeley. His research interest is mainly focused to microfluidics applications in diagnostics and biotechnology. He is also serving as CTO in the Fluidlab startup.

Jure Derganc is the Head of the Institute of Biophysics at the Faculty of Medicine, University of Ljubljana. He holds a PhD in Physics from the University of Ljubljana. His research interests include the synthetic biology of membranes, cell biophysics, and the biomedical applications of microfluidics.